Supercritical carbon dioxide spray drying for the production of stable dried protein formulations

Nuchuchua, O.

CHAPTER 2

Characterization of drug delivery particles produced by supercritical carbon dioxide technologies

Onanong Nuchuchua[1], M. Reza Nejadnik[1], Sebastiaan C Goulooze[2], Nataša Jovanović Lješković[3], Hayley Ann Every[4], Wim Jiskoot[1]

[1] Division of Drug Delivery Technology, Cluster Biotherapeutics, Leiden Academic Centre for Drug Research (LACDR), Leiden University, The Netherlands

[2] Division of Pharmacology, Leiden Academic Centre for Drug Research (LACDR), Leiden, The Netherlands

[3] Department of Pharmaceutics, Utrecht Institute for Pharmaceutical Sciences, Utrecht, The Netherlands

[4] FeyeCon Development & Implementation B.V., Weesp, The Netherlands

*Submitted in J. Supercrit. Fluid.

Abstract

This review focuses on characterization methods for drug/excipient particles produced with supercritical CO_2 ($scCO_2$) particle engineering technologies. Proper characterization of particles can guide optimization of their production process and provide an indication of their *in vivo* behavior. In particular, characterization techniques for particle size distribution and morphology, drug loading and release, structure of matrix components, biotherapeutic activity, porosity analysis, particle surface, surface charge, toxicology/biocompatibility and residual solvent/water analysis, are discussed. Moreover, we discuss particle analytical techniques that are not commonly used in the $scCO_2$ research field but are of potential use for pharmaceutically relevant $scCO_2$-engineered particles. These techniques often work synergistically in particle characterization by mutually supporting the interpretation of their outcomes, which is crucial to efficiently develop a successful production process of drug/excipient particles.

1. Introduction

Therapeutic agents, such as small molecules, proteins and vaccines are often formulated in a matrix that may consist of biopolymers, sugars, polysaccharides, porous materials (e.g., silica) or inorganic compounds. The preparation of these matrices in particle form has been shown to improve drug delivery in several ways, e.g., by allowing the use of less invasive administration routes, improving drug stability, controlling the release profile, increasing bioavailability and/or selectively targeting of particular tissues or cell types [1-3]. Some pharmaceutical particle products have already obtained market approval and are currently used in established treatments of diseases [4]. One example is an anticancer agent, formulated as paclitaxel/albumin nanoparticles with improved solubility and delivery of the drug into endothelial cells when compared to traditional paclitaxel formulations [5].

Various characteristics of the particles have been shown to greatly influence the performance of the particulate formulation. Particle size, among others, is of significance in the process of drug administration, where typically particles with a size range between 0.1-0.3 µm are used for intravenous (IV) delivery, 10-200 µm for subcutaneous or intramuscular delivery [6], 1-5 µm for pulmonary delivery and 0.1-100 µm for oral delivery [7]. In most cases, particles have to reach their target site through the blood circulation system. After entering the vascular bed, particles can escape from the circulation through openings, also called fenestrations, of the endothelial barrier. The size limits of these openings for different organs has been summarized elsewhere and is a contributing factor to the typical particle size dependent biodistribution of particles in the body. Although it is roughly said that particles have to be smaller than 150 nanometer to cross the endothelial barrier, there are several reports that indicate penetration of particles much larger than the limits of these opening [8]. These observations have mainly to do with pathological conditions where the vasculature and the fenestrations undergo changes in size and allow penetration of larger particles. For instance nanoparticles as large as a couple of hundred nanometer in diameter have been used to target tumor cells [9, 10]. In a different area of application, the particle size is a critical factor in induction of immunogenicity in vaccine delivery systems [11, 12]. Briefly, nanoparticles target the $CD8^+$ T cell responses and dendritic cells while microparticles (2-3 µm) activate macrophages. Size is just one attribute of particle characteristics and there is a vast amount of information concerning the relevance of other properties of particles in various pharmaceutical applications.

The above-mentioned relations between the particle characteristics and their window of potential function indicate that, regardless of the application, the engineering of particles for drug delivery requires comprehensive characterization of the physical, chemical and biological attributes of the particles. A good characterization provides required data for understanding the property-function relations and for the optimization of particle production processes and therapeutic efficacy. Thus, careful selection of characterization techniques is crucial for the development of stable and effective drug delivery particles.

Particle preparation for pharmaceutical applications is typically carried out by conventional techniques, such as milling, solvent evaporation and spray drying [13], or relatively new methods such as supercritical carbon dioxide technology, cryogenic technologies, and nanomilling [14]. Milling involves the use of a mechanical force to break up a material into smaller particles, typically in the range of 1-100 μm. While such methods are inexpensive, the particle size and homogeneity that can be achieved are often limited [15]. Particle formation by solvent evaporation is a simple method for preparing particles over a broad size range. However, residual solvents can remain in the particles [16], which may lead to cytotoxicity upon administration. Spray drying produces powder product by atomizing a solution to form droplets that are subsequently dried by hot air. While it is a fast and easily scalable process that is capable of achieving narrow particle size distributions in the range of 0.1 to 1000 μm, the high temperatures needed for drying can lead to degradation of biological compounds [17-19]. Cryogenic technologies, such as freeze drying, rely on sublimation to produce dried products. They are considered to be a mild process and are generally used for the dehydration of biotherapeutics. However, the particle size of freeze-dried products is not well-controlled. Moreover, such methods are energy intensive and time consuming [20].

Among these techniques, the use of supercritical CO_2 ($scCO_2$) to create multicomponent drug/excipients particles is of particular interest for several reasons [21]. $ScCO_2$ has a relatively mild critical pressure (7.4 MPa) and temperature (301.4 K), allowing processing of thermolabile substances at desirable temperatures [22-24]. It is also inexpensive, nontoxic and relatively inert [25].

Moreover, $scCO_2$ technology can be used to process a broad range of drug formulations from a variety of materials with controlled size distributions and specific particle morphologies [21, 26-29], in particular to develop drug carrier systems [26, 30, 31] and to improve drug

bioavailability [32]. A review article of Campardelli et al. [31] introduced several $scCO_2$-based particle production techniques that allow for preparation of solid nanoparticles, nanostructured and nanoporous microparticles, and nanoporous materials. The literature cited in this review demonstrates that there is a large, heterogeneous array of particles for pharmaceutical applications that have been engineered by using $scCO_2$ technology [33]. These particles have been characterized by various techniques and literature data show that the methods used to characterize drug/excipient particles are numerous and aiming for a broad range of properties, while no standard testing procedure has been implemented (Table 1 and Fig. 1). Moreover, it is apparent from these articles that the influence of the processing conditions in $scCO_2$ processes on the resultant particle characteristics is not well understood, compared to conventional particle production methods.

The aim of this review is to discuss the strategies and methods used for the characterization of $scCO_2$-produced drug-containing particles. In particular, the techniques are categorized with respect to their targeted properties, i.e., particle size distribution and morphology, drug loading and release, structure of matrix components, biotherapeutic activity, surface chemistry, porosity, surface charge, toxicology/biocompatibility and residual solvent/water. This review will take into consideration the strengths and weaknesses of each characterization technique, and also include a list of methods that may potentially be useful as additional characterization methods for particles produced with $scCO_2$ technology. Table 2 summarizes techniques that have been used to characterize particles prepared by $scCO_2$ technologies (indicated by an asterisk when such a technique is used in one of the cited articles in Table 1) as well as techniques that have been used for particles prepared with other methods and can be useful for characterizing drug-containing particles engineered by $scCO_2$ technologies. In the review of each technique special attention will be paid to highlighting the way characterization can help improving the production and application of particulate drug delivery systems.

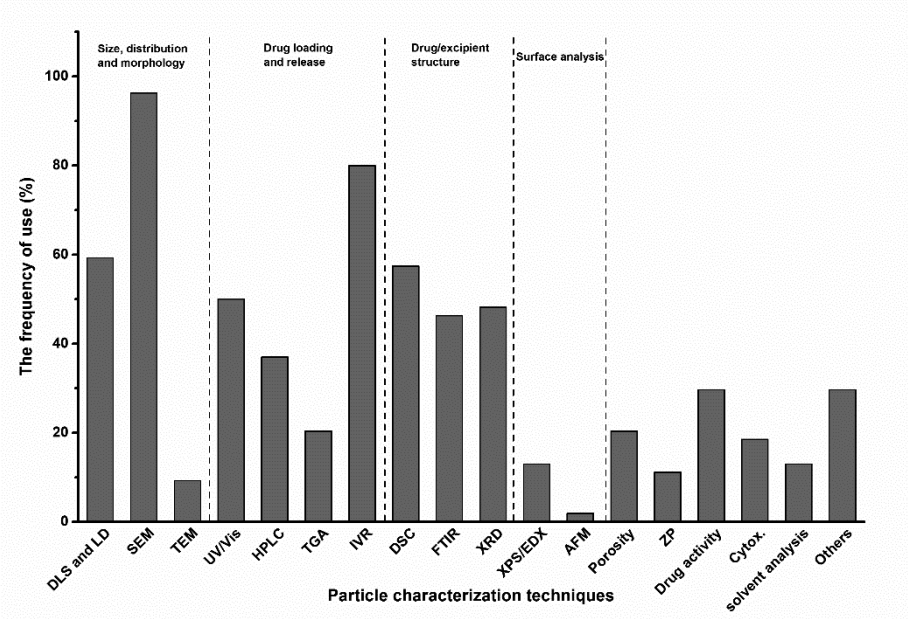

Fig. 1 The frequency of use of particle characterization techniques used in $scCO_2$ technology. Abbreviations; **AFM** (Atomic force microscopy), **Cytox** (Cytotoxicity by in vitro and in vivo assay), **DLS and LS** (dynamic light scattering and laser diffraction), **DSC** (Differential scanning calorimetry), **EDX** (Energy dispersion X-ray spectroscopy), **FTIR** (Fourier transform infrared spectroscopy), **HPLC** (high performance liquid chromatography with UV detector), **IVR** (*In vitro* release and dissolution study), **Porosity** (Brunauer-Emmett-Teller surface area analysis and Barrett-Joyner-Halenda determination, N_2 absorption and pore size distribution), **SEM** (Scanning electron microscopy), **Solvent analysis** (Gas chromatography), **TGA** (Thermogravimetric analysis), **TEM** (Transmission electron microscopy), **UV/Vis** (UV/Vis spectroscopy), **XPS** (X-ray photoelectron spectroscopy), **XRD** (X-ray diffraction), and **ZP** (Zeta potential measurement).

Table 1. Particle characterization techniques used in the field of $scCO_2$ techniques.

Particle constituents	Role CO_2 (production technique)	Particle size distribution, morphology				Drug loading and release				Structure of drug/excipient			Surface chemistry	Refs.
		LS/ LD	SEM	TEM	NTA/MFI	UV/Vis	TGA	IVR	HPLC/ UV	DSC	FTIR	XRD	XPS/EDX	
Retinyl palmitate, PLA	**Solvent** (RESOLV)	•	•			•								[84]
Fenofibrate, PLGA	**Solvent** (RESOLV)	•	•							•		•		[148]
Naproxen, PLA	**Solvent** (RESS)	**SMPS**	•								•			[118]
Prednisolone, PEG, SDS	**Non-solvent** (ASES)	•	•											[171]
Lysozyme, PLA, ammonium bicarbonate	**Non-solvent** (emulsion-combined PCA)	•	•			•	•	•		•	•			[64]
Methotrexate, PLA	**Non-solvent** (emulsion-combined PCA)	•	•			•		•		•	•	•		[65]
Curcumin, PLGA	**Non-solvent** (fluidization-assisted SAS)	•	•			•		•		•				[79]
5-fluorouracil, PLA-PEG, PEG	**Non-solvent** (reverse emulsion SEDS)	•	•				•	•	•		•			[63]
Azacitidine, PLA	**Non-solvent** (SAS)		•					•	•	•				[172]
Gentamicin, PVP/MA	**Non-solvent** (SAS)		•								•			[114]
Nilotinib, HPMCP	**Non-solvent** (SAS)	•	•					•	•	•		•		[130]
Paracetamol, PLA	**Non-solvent** (SAS)		•	•				•		•		•	•	[13]
Paracetamol, PLA	**Non-solvent** (SAS)		•				•	•						[173]
Dutasteride, HP-β-CD	**Non-solvent** (SAS)	•	•						•			•		[174]

Cilostazol and one of (Poloxamer 188, Poloxamer 407, TPGS 1000, Gelucire® 44/14, Gelucire ® 50/13)	**Non-solvent** (SAS)	•	•					•	•	•	•	•		[175]
Amoxicillin, ethyl-cellulose	**Non-solvent** (SAS)		•			•		•	•				•	[137]
Camptothecin, folic acid conjugated dextran	**Non-solvent** (SAS)	•	•			•			•	•	•	•		[176]
Diflunisal, PVP	**Non-solvent** (SAS)		•				•	•		•	•	•		[132]
Quercetin, poloxamer 407	**Non-solvent** (SAS)		•			•		•		•	•	•		[156]
10-hydroxycamptothecin, PLA	**Non-solvent** (SAS)			•				•	•	•	•	•		[131]
Lysozyme, $CaCO_3$	**Non-solvent** (SAS)	•	• **OM**						•			•		[150]
Viscumin, PLA	**Non-solvent** (ultrasound-assisted SAS)		•			•		•						[177]
Curcumin, PLGA	**Non-solvent** (ultrasound-assisted SAS)	•	•			•				•		•		[178]
Rifampicin, lactose	**Non-solvent** (SAS-DEM)		•			•				•	•	•		[49]
Nevirapine, lactose,	**Non-solvent** (SAS-DEM)	•	•			•		•		•	•	•		[51]

microcrystalline cellulose														
Itraconazole, lactose	**Non-solvent** (SAS-DEM)	**LO**	•			•		•		•	•			[50]
Paclitaxel, PLA	**Non-solvent** (SAS-EM)		•					•	•	•				[48]
One of (piroxicam and diclophenac), PLGA	**Non-solvent** (SFEE)	•	•	•		•		•				•	•	[43]
Insulin, PLGA	**Non-solvent** (SFEE)	•	• **OM**					•	•					[44]
Piroxicam, PLGA	**Non-solvent** (SFEE)	•	• **OM**			•		•		•			•	[39]
Hydrocortison, PLGA	**Non-solvent** (SFEE)	•	• **OM**			•		•		•				[42]
Rhodamine, hollow gold nanoshells, PLA	**Non-solvent** (SFEE)	•	•	•		•		•	•				•	[135]
Morphine, PLA-PEG-PLA	**Non-solvent** (SEDS)	•	•			•		•			•	•		[179]
Indomethacin, Fe_3O_4, PLA	**Non-solvent** (SEDS)	•	•				•				•		•	[85]
Paclitaxel, PLA	**Non-solvent** (SEDS)	•	•	•				•	•	•		•		[89]
Indomethacin, PLA, PLGA	**Non-solvent** (SEDS)	•	•			•		•		•	•	•		[110]
Amoxicillin, chitosan	**Non-solvent** (SEDS)	•	•			•		•		•		•		[111]
Puerarin, PLA	**Non-solvent** (SpEDS)		•			•		•			•			[61]
5-fluorouracil, SiO_2, PLA	**Non-solvent** (SpEDS)	•	•			•	•			•	•			[62]
Methotrexate, PLA-PEG-PLA	**Non-solvent** (SpEDS)		•			•		•			•			[60]

Methotrexate, Fe_3O_4, PLA-PEG-PLA	**Non-solvent** (SpEDS)		•	•		•	•	•		•	•		•	[88]
Fenofibrate, SBA-15	**Solvent/ non-solvent** $scCO_2$-assisted impregnation		•				•	•	•	•		•	•	[134]
Fenofibrate, SBA-15	**Solvent/ non-solvent** $scCO_2$-assisted impregnation						•	•	•	•	•	•		[124]
Metronidazole, melanin	**Solvent/ non-solvent** $scCO_2$-assisted impregnation		•			•		•			•	•		[180]
Ibuprofen, DMAEMA-based molecularly imprinted polymers	**Solvent/ non-solvent** $scCO_2$-assisted impregnation		•					•						[181]
Ibuprofen, MCM-41	**Solvent/ non-solvent** $scCO_2$-assisted impregnation		•			•	•	•		•		•		[120]
Fenofibrate, Neusilin UFL2	**Solute** Melt-adsorption		•						•	•		•	•	[59]
Tetanus Toxoid, PLA	**Solute** PGSS	•	•			•		•	**SEC**					[53]
hGH, PLA, PLGA	**Solute** PGSS	•	•					•	**SEC**					[54]
BSA (bovine serum albumin), one of(PLA, PLA-PEG copolymers)	**Solute** PGSS	•	•			•		•		•				[55]
S-(+)-ibuprofen, one or	**Solute** PGSS	•	•					•	•					[182]

several of (Pluronic® F127, Pluronic® L64, Gelucire®, glyceryl monostearate)														
Gentamicin, dextran	**Atomization aid** SAA	•	•				•	•	•	•	•			[74]
Gentamicin, heat denatured albumin	**Atomization aid** SAA	•	•					•	•	•	•	•		[75]
Lyosozyme, myoglobin, trehalose, sucrose	**Atomization aid**		•							•	•	•		[67, 116]
Polyclonal human serum IgG, trehalose, cyclodextrin	**Atomization aid**										•			[117]
Lysozyme, a-lactalbumin, a-chymotrypsinogen A, monoclonal antibody, myoglobin Trehalose	**Atomization aid**		•			•	•		**SEC**	•				[68, 69]
Piroxicam, PVP	**Other** Polymerization medium/solvent		•			•		•			•	•		[183]

Table 1. Particle characterization techniques used in the field of $scCO_2$ techniques (continue).

Particle constituents	Role CO_2 (production technique)	Porosity	Surface charge	Drug activity	Toxicology	Residual solvent and water content	Other properties*	Refs.
		BET and BJH/N_2 absorption/Pore size distribution	**ZP**		***In vitro* and *In vivo***	**GC and Karl Fischer method**		
Retinyl palmitate, PLA	**Solvent** (RESOLV)							[84]
Fenofibrate, PLGA	**Solvent** (RESOLV)		•					[148]
Naproxen, PLA	**Solvent** (RESS)							[118]
Prednisolone, PEG, SDS	**Non-solvent** (ASES)							[171]
Lysozyme, PLA, ammonium bicarbonate	**Non-solvent** (emulsion-combined PCA)	**HPMIP**		•			•	[64]
Methotrexate, PLA	**Non-solvent** (emulsion-combined PCA)	**HPMIP**		•	•	•	•	[65]
Curcumin, PLGA	**Non-solvent** (fluidization-assisted SAS)							[79]
5-fluorouracil, PLA-PEG, PEG	**Non-solvent** (reverse emulsion SEDS)			•	•			[63]
Azacitidine, PLA	**Non-solvent** (SAS)							[172]
Gentamicin, PVP/MA	**Non-solvent** (SAS)			•	•		•	[114]
Nilotinib, HPMCP	**Non-solvent** (SAS)		•	•		•	•	[130]
Paracetamol, PLA	**Non-solvent** (SAS)							[13]
Paracetamol, PLA	**Non-solvent** (SAS)		•					[173]
Dutasteride, HP-β-CD	**Non-solvent** (SAS)	•		•			•	[174]
Cilostazol and one of	**Non-solvent** (SAS)	•				•	•	[175]

(Poloxamer 188, Poloxamer 407, TPGS 1000, Gelucire® 44/14, Gelucire ® 50/13)								
Amoxicillin, ethyl-cellulose	**Non-solvent** (SAS)							[137]
Camptothecin, folic acid conjugated dextran	**Non-solvent** (SAS)							[176]
Diflunisal, PVP	**Non-solvent** (SAS)							[132]
Quercetin, poloxamer 407	**Non-solvent** (SAS)			•				[156]
10-hydroxycampto thecin, PLA	**Non-solvent** (SAS)							[131]
Lysozyme, $CaCO_3$	**Non-solvent** (SAS)		•	•				[150]
Viscumin, PLA	**Non-solvent** (ultrasound-assisted SAS)				•			[177]
Curcumin, PLGA	**Non-solvent** (ultrasound-assisted SAS)							[178]
Rifampicin, lactose	**Non-solvent** (SAS-DEM)							[49]
Nevirapine, lactose, microcrystalline cellulose	**Non-solvent** (SAS-DEM)							[51]
Itraconazole, lactose	**Non-solvent** (SAS-DEM)	•						[50]
Paclitaxel, PLA	**Non-solvent** (SAS-EM)							[48]
One of (piroxicam and diclophenac), PLGA	**Non-solvent** (SFEE)					•		[43]

Insulin, PLGA	**Non-solvent** (SFEE)			•	•			[44]
Piroxicam, PLGA	**Non-solvent** (SFEE)					•		[39]
Hydrocortison, PLGA	**Non-solvent** (SFEE)					•		[42]
Rhodamine, hollow gold nanoshells, PLA	**Non-solvent** (SFEE)							[135]
Morphine, PLA-PEG-PLA	**Non-solvent** (SEDS)						•	[179]
Indomethacin, Fe_3O_4, PLA	**Non-solvent** (SEDS)				•		•	[85]
Paclitaxel, PLA	**Non-solvent** (SEDS)		•	•	•			[89]
Indomethacin, PLA, PLGA	**Non-solvent** (SEDS)			•	•		•	[110]
Amoxicillin, chitosan	**Non-solvent** (SEDS)			•			•	[111]
Puerarin, PLA	**Non-solvent** (SpEDS)							[61]
5-fluorouracil, SiO_2, PLA	**Non-solvent** (SpEDS)							[62]
Methotrexate, PLA-PEG-PLA	**Non-solvent** (SpEDS)							[60]
Methotrexate, Fe_3O_4, PLA-PEG-PLA	**Non-solvent** (SpEDS)					•	•	[88]
Fenofibrate, SBA-15	**Solvent/ non-solvent** $scCO_2$-assisted impregnation	•						[134]
Fenofibrate, SBA-15	**Solvent/ non-solvent** $scCO_2$-assisted impregnation	•						[124]
Metronidazole, melanin	**Solvent/ non-solvent** $scCO_2$-assisted impregnation				•		•	[180]

Ibuprofen, DMAEMA-based molecularly imprinted polymers	**Solvent/ non-solvent** $scCO_2$-assisted impregnation	•	•		•		•	[181]
Ibuprofen, MCM-41	**Solvent/ non-solvent** $scCO_2$-assisted impregnation	•						[120]
Fenofibrate, Neusilin UFL2	**Solute** Melt-adsorption	•		•				[59]
Tetanus Toxoid, PLA	**Solute** PGSS			•			•	[53]
hGH, PLA, PLGA	**Solute** PGSS			•			•	[54]
BSA (bovine serum albumin), one of(PLA, PLA-PEG copolymers)	**Solute** PGSS							[55]
S-(+)-ibuprofen, one or several of (Pluronic® F127, Pluronic® L64, Gelucire®, glyceryl monostearate)	**Solute** PGSS							[182]
Gentamicin, dextran	**Atomization aid** SAA			•			•	[74]
Gentamicin, heat denatured albumin	**Atomization aid** SAA							[75]
Lyosozyme, myoglobin, trehalose, sucrose	**Atomization aid**			•		•	•	[67, 116]
Polyclonal human serum	**Atomization aid**						•	[117]

IgG, trehalose, cyclodextrin								
Lysozyme, α-lactalbumin, α-chymotrypsinogen A, monoclonal antibody, myoglobin Trehalose	**Atomization aid**			•		•	•	[68, 69]
Piroxicam, PVP	**Other** Polymerization medium/solvent							[183]

BET/BJH (Brunauer-Emmett-Teller surface area analysis and Barrett-Joyner-Halenda determination), **DSC** (Differential scanning calorimetry), **EDX** (Energy dispersion X-ray spectroscopy), **FTIR** (Fourier transform infrared spectroscopy), **GC** (Gas chromatography), **HPLC/UV** (high performance liquid chromatography with UV detector), **HPMIP** (High-pressure mercury intrusion porosimetry), **IVR** (*In vitro* release and dissolution study), **LD** (Laser diffraction), **LS** (Light scattering techniques), **LO** (Light obscuration), **MFI** (Flow-imaging microscopy), **NTA** (Nanoparticle tracking analysis), **OM** (Optical microscopy), **Others** (mucoadhesion, particle stability, residual water/organic content determination, protein structure analysis), **SEC** (Size exclusion chromatography), **SEM** (Scanning electron microscopy), **SMPS** (Scanning mobility particle sizer), **TEM** (Transmission electron microscopy), **TGA** (Thermogravimetric analysis), **UV/Vis** (UV/Vis spectroscopy), **XRD** (X-ray diffraction), **XPS** (X-ray photoelectron spectroscopy), **ZP** (Zeta potential measurement).

2. Supercritical carbon dioxide-mediated particle engineering

2.1. $scCO_2$ as a solvent

Several methods use $scCO_2$ as a solvent for drug and/or excipient, and rely on a reduction in pressure to induce particle formation. The first method of this category is often referred to as the Rapid Expansion of Supercritical Solutions (RESS) technique [34]. After the constituents are dissolved in $scCO_2$, the mixture is depressurized over a nozzle. The resulting expansion of $scCO_2$ reduces its solvation power, leading to supersaturation of the mixture and precipitation of the solute to form particles. The use of this technique is often limited, as $scCO_2$ remains a poor solvent for most of the polymers and pharmaceutical compounds, making RESS-like processes a less viable option for the production of particles containing them [33].

One way to overcome the limited solubility is by using an organic co-solvent, which can be added to increase the solubility of drug or polymer in the $scCO_2$. However, when working with organic solvents, there is the risk that some solvent remains in the particles, therefore requiring additional drying steps to remove it. Moreover, the solvent may also cause particle agglomeration [33]. Variations of the RESS method include a non-solvent RESS process (RESS-N), which relies on the differences in solubility of an excipient and drug in $scCO_2$ to promote the precipitation of the excipient on the already prepared drug particles to create microparticles with a core-shell structure [35-37], and the spraying of the supercritical solution into a liquid solvent (RESOLV), to obtain a suspension of micro- or nanosized particles [33, 38].

The second technique that makes use of $scCO_2$ as a solvent is $scCO_2$-assisted impregnation. When a saturated solution of drug in $scCO_2$ is brought into contact with insoluble excipient particles, the drug can be loaded into the particles by two mechanisms [39]. In the first approach, rapid depressurization of the $scCO_2$/drug solution allows for the drug to be deposited inside the particles, which often consist of a polymer or silica matrix. During such a process, it is possible that the drug can deposit outside the excipient particles, leading to an inhomogeneous mixture of drug and excipient molecules. The second mechanism involves drug adsorption by the excipient, which relies on an interaction (e.g., H-bonding) between the solid excipient particles and the drug [39]. When the excipient is a polymer, $scCO_2$ serves not only as a solvent for the drug, but also promotes diffusion of the $scCO_2$ solution into the polymer matrix by swelling of the polymer[40].

In the third method, that is Supercritical Fluid Emulsion Extraction (SFEE) technique, a $scCO_2$ solvent can be used to dissolve and extract the organic phase of an emulsion. In this case, the drug and other particle constituents are dissolved in the organic phase of a traditional oil-in-water emulsion and $scCO_2$ is a non-solvent for the particle constituents that can extract the organic solvent very rapidly and efficiently. The extraction of the organic phase will produce an aqueous suspension of microparticles, which can subsequently be filtered and dried to obtain a powder. One of the benefits of SFEE is that the particle size can be controlled by manipulating the size of the droplets in the emulsion [41]. In addition, the aqueous phase is supposed to prevent agglomeration [41]. This method was originally developed by Shekunov et al. [42] for the preparation of pure nanoparticles of cholesterol acetate, griseofulvin and megestrol. It has also been used to create drug/polymer particles with Eudragit® and poly(lactic-co-glycolic acid)(PLGA) [41, 43-46].

2.2. $scCO_2$ as a non-solvent

The fact that most drugs and polymers have a poor solubility in $scCO_2$ can also be exploited in particle formation techniques, where the $scCO_2$ is then used as an anti-solvent. In processes like Supercritical Anti-Solvent (SAS) and Precipitation with Compressed Anti-solvent (PCA), a solution of drug and excipients is sprayed into a precipitation chamber containing $scCO_2$ [47]. As the $scCO_2$ dissolves into the sprayed droplets, the solubility of the constituents in the droplet decreases, leading to the precipitation of micro- or nanosized particles [48]. These anti-solvent processes often lead to very small (down to nm size range) particles, as the rapid precipitation limits the possibility for the particles to grow. However, an additional organic solvent is often employed in anti-solvent processes to enhance the mass transfer between $scCO_2$ and drug/excipient solution, leading to remaining of a residual organic solvent content in particles [47], which may cause cytotoxicity upon drug administration.

Several modifications of the $scCO_2$ anti-solvent process have been developed, to improve the atomization and to create particles with narrower size distributions. Chattopadhyay et al. [49] developed the Supercritical Anti-Solvent with Enhanced Mass Transfer (SAS-EM) process, where an atomizing tip with ultrasonic frequency is used to improve mass transfer between $scCO_2$ and the drug/excipient solution. The same technique was used by Lee et al. [50] to produce microparticles of paclitaxel and poly L-lactic acid (PLA). In a variation of this method called the Supercritical Anti-Solvent Drug-Excipient Mixing (SAS-DEM)

process, a drug solution is sprayed into a suspension of excipients in $scCO_2$. This causes the drug to precipitate in composite particles containing the excipient. This method is used to avoid agglomeration of drug particles and improve the dissolution rate by increasing the surface area [51-53].

2.3. $scCO_2$ as a solute

$scCO_2$ can dissolve in many polymeric matrices, causing swelling and lowering of the glass transition temperature [47]. This behavior is exploited in the Particles from Gas Saturated Solutions (PGSS) process, as it allows for intimate mixing of a molten polymer and an (insoluble) drug. Subsequent rapid depressurization of the $scCO_2$ saturated molten mixture over a nozzle causes a rapid and homogeneous cooling of the sample, which induces precipitation of solid drug/polymer particles [54]. This method has been used recently to make protein/polymer particles with several different polymers such as PLGA, PLA and copolymers of PLA and polyethylene glycol (PEG) [55-57]. In addition, the PGSS technique has been used to prepare protein-loaded lipid-based particles with a high protein loading and a controlled released profile [33, 58]. In this case, the technique has been referred to as Gas-Assisted Melting Atomization (GAMA). Despite the ability of the process in producing particles, it has been reported that the PGSS process is disadvantageous for preparation of particles in the submicron size range [59].

Moreover, $scCO_2$ can help to improve a traditional hot-melting dispersion method for manufacturing micronized particles, by lowering the melting temperature of dispersed active agents [60]. As shown in a study by Cha et al. [61], the suppression in melting by the supercritical allows for intimate mixing between a molten drug (fenofibrate) and a mesoporous carrier (magnesium aluminometasilicate, Neusilin UFL2) at only 50 °C, in contrast to the hot-melting method, which was conducted at 90 °C.

2.4. $scCO_2$ as a drying medium

In a commonly used technique called Solution-Enhanced Dispersion by $ScCO_2$ (SEDS), the solution is mixed with $scCO_2$ prior to spraying through a coaxial nozzle [33]. This increases the mass transfer between the sprayed solution and $scCO_2$, reducing both the drying time and the extent of particle agglomeration. Alternatively, a similar $scCO_2$/solution mixture can be sprayed into a liquid phase, to create a dispersion as in the case of Suspension Enhanced Dispersion by $scCO_2$ (SpEDS) [62-64]. Another modification of the SEDS technique was developed by Zhang et al. [65]: the reverse-emulsion-Solution Enhanced

Dispersion by $scCO_2$ (reverse emulsion-SEDS), in which an oil-in-water emulsion containing both drug (5-fluorouracil) and polymer was dried using an SEDS-like process. However, the emulsion sprayed into the $scCO_2$ medium was not treated with $scCO_2$ prior to spraying. The reverse emulsion-SEDS is also comparable to the emulsion-combined PCA [66, 67].

Similar to the SEDS process, $scCO_2$ is used as a low temperature drying medium, which is particularly beneficial for thermolabile substances [68]. In the $scCO_2$ spray drying process, a protein formulation is pumped into the drying system, where it is atomized by the $scCO_2$ via a nozzle into a drying vessel filled with $scCO_2$ [69]. The water removal from the atomized droplets is carried out in the vessel by mass transfer between water and $scCO_2$ phases. The $scCO_2$ spray drying has been used to prepare dried formulations of lysozyme [69], myoglobin [69, 70] and immunoglobulin G [71] in our laboratories. The two other techniques in this category are $scCO_2$ assisted atomization (SAA) and carbon dioxide-assisted nebulization with a bubble dryer (CAN-BD) [72, 73]. In both cases, $scCO_2$ is mixed with a solution of the drug/polymer prior to spraying, to create either an emulsion or a solution. The emulsion/solution is then sprayed into a vessel at lower pressure, where the expansion of $scCO_2$ facilitates the formation of microdroplets, allowing for fast drying (several ms) despite the low temperatures (32 - 52 °C) [74, 75]. The SAA technique has been used recently to create gentamicin/albumin particles and gentamicin/alginate/pectin particles [76, 77]. SAA and CAN-BD processes are similar to PGSS drying for preparing particles of β-carotenoid in lecithin as described by Paz et al. [78]. It has been suggested that proteins can suffer from an acidification by CO_2, however, a suitable buffer can control the pH of protein formulations during $scCO_2$ drying processes [70].

3. Particle characterization

The order of the presentation of particle characterization techniques that are discussed in this review paper is based on the frequency of their use for the analysis of $scCO_2$ engineered particles. As presented in Fig. 1, more that 50% of the analyses by particle characterization methods have aimed for investigating one of these three categories of properties: 1) particle size distribution and morphology, 2) drug loading and release and 3) drug and excipient structure. Other properties such as surface chemistry and charge, *in vitro* and *in vivo* drug activity and efficacy, toxicology and others have been less studied.

3.1. Particle size distribution and morphology

3.1.1. Dynamic light scattering (DLS) and laser diffraction (LD)

Dynamic light scattering (DLS) or photon correlation spectroscopy measures the variation of the intensity of scattered light over time to determine the diffusion coefficient and therewith the average equivalent-sphere hydrodynamic diameter of particles in a suspension [79, 80]. This technique can measure particle size in the range of about 1-1000 nm. DLS measurements are easy to perform and this technique is quite common due to the availability of the necessary equipment in most laboratories. However, small traces of large particles and agglomerates can skew the results, because they scatter light more efficiently than smaller particles do [8].

DLS analysis was applied to study the effects of the production parameters of the SAS process with ultrasonic vibration to prepare uniform PLGA-coated curcumin nanoparticles in the range of 40-63 nm. The results showed that low power of the ultrasonication (60 W) resulted in poor mixing of pure curcumin particles, whereas curcumin aggregation occurred with a high ultrasonic power (420 W) [81]. Another study by Zhang et al. [65] used DLS to determine influences of operating parameters of a reverse-emulsion SEDS process on the particle size distribution of 5-fluorouracil (an antitumor drug) loaded in a copolymer PLA/PEG. The results suggested that the nanoparticles with a narrow size distribution were obtained when the pressure of the SEDS process was high, but the operational temperature and solution flow rate were low. In this study, the DLS results were supported by the images from scanning electron microscopy (SEM).

Laser diffraction (LD), similar to DLS, is based on analysis of the scattered light. It is in principle a commonly used static light scattering method in which particle sizes are determined based on an intensity of scattered light as a function of scattering angle. LD is suitable for measurement of the particle size in the range of submicron to millimeter. LD has been used in studies of Kang et al. [66] and Chen et al. [67] to observe drug-loaded, porous PLA microparticles prepared by PCA process. The particles were designed for pulmonary drug delivery. In theory, inhaled drug/excipient particles should have an aerodynamic diameter (aerodynamic diameter is a function of geometric size and particle density) in a range of 1-5 μm to reach the alveolar airways [82]. The results of the LD measurement suggested that the geometric particle sizes of drug-loaded porous microparticles were about 10-20 μm. However, due to the porosity of particles resulting in a lower density, the aerodynamic diameter of drug-loaded PLA porous microparticles was

about 3 μm [66, 67]. Therefore, porous particles with a geometric size greater than 10 μm may have a desired aerodynamic size due to the low mass densities of particles [83, 84].

3.1.2. Scanning electron microscopy (SEM)

SEM is used to visualize the morphology or shape of particles in a dry state. SEM uses a focused beam of electrons to scan the sample. Various types of signals (secondary or back-scattered electrons and X-rays) coming from the sample can be detected to create an image, or gain information about the elemental composition of the surface. The resolution of a SEM image can be as small as 1 nm [85], while at the lowest magnification particles as large as hundreds of microns can be imaged. Based on SEM images, Sane and Limtrakul [86] showed that PLA nanoparticles loaded with a model drug (retinyl palmitate) from RESOLV process were different in size due to presence or absence of a component of retinyl palmitate and excipients in the precipitating solution. SEM also gave clear images of the agglomerates of retinyl palmitate/PLA nanoparticles. However, particles seen in SEM images are dry and therefore their size can be smaller than their hydrodynamic diameter determined from DLS or some other light interaction methods [86]. Moreover, SEM images can be also used for estimation of particle porosity and the elemental analysis of a particle surface [41, 52, 87], as explained below.

3.1.3. Transmission electron microscopy (TEM)

Using TEM, particles with a size range of 1 nm - 5 μm can be imaged [88]. The intensity of electrons after interacting to a specimen is detected at the other side of the sample, and then used to create a sample image [89]. Although better resolutions can be achieved with TEM (0.1 nm) than with SEM, the sample preparation tends to be more complex. TEM is also used to visualize the distribution of the constituents in particles and distribution of particles after uptake [13, 90, 91]. It is noteworthy that the use of a focused electron beam in TEM may damage the structure of material samples during the imaging.

A few examples of TEM for particle engineered by $scCO_2$ processes are available (see Table 1). TEM micrographs have been used to observe the internal structure of particles, e.g., to evaluate whether there are pores or localized structures in particles that indicate effective loading with a drug. Kalani and Yunus [13] showed the 15.5 nm thickness of a PLA outer shell filled with paracetamol inside, after coprecipitating in antisolvent CO_2 process. In addition, the TEM can be coupled with energy dispersion X-ray spectroscopy in order to analyze presence of

elements from a drug and excipient in nanoparticles prepared by Suspension-Enhanced Dispersion by Supercritical CO_2 (SpEDS), which is a modified version of the SEDS process mentioned in section 2.4 [90].

3.1.4. Optical microscopy (OM)

The use of visible light to magnify an object by an objective and eyepiece lens is probably the oldest particle characterization technique for micron sized particles. OM has been applied for observing the formation of the $water_1/oil/water_2$ emulsion of drug/PLGA microspheres [41, 44]. The primary $water_1/oil$ emulsion consisted of a water phase (a drug suspension in a solution of polyvinyl alcohol (PVA) in ethanol or DMSO) in an oil phase (PLGA in ethyl acetate), while the secondary $water_2$ solution was ethyl acetate-saturated aqueous PVA solution. The emulsion was later introduced into the supercritical fluid emulsion extraction (SFEE). After depressurization, the microspheres were formed while residual organic solvents in the $water_1/oil/water_2$ emulsion were extracted. The images of OM can be used for simple and fast screening of emulsion droplet formation. However, other techniques such as SEM or TEM may be required to observe more details of particle morphology [41, 44].

3.1.5. Nanoparticle tracking analysis (NTA)

NTA analyzes particles in liquid solutions using the visualization of the light scattered by single particles and tracking of the Brownian motion of those particles. The instrument consists of a laser light scattering microscope with a charge-coupled device (CCD) camera, which enables the visualization and recording of the movement of nanoparticles in suspension, and a software, which will track and identify individual nanoparticles moving under Brownian motion and relates the movement to a particle size according to the Stokes-Einstein equation. This technique is suitable for particle sizes between 30 and 1000 nm, and particle concentrations in the range of 10^7–10^9/ml [92]. The measurement requires a small amount of a sample solution (less than 1 ml).

In a study of Nuchuchua et al. [71], NTA was used to determine of the nanoparticle size distribution and concentration in the reconstituted samples of dried protein/trehalose formulations prepared by $scCO_2$ spray drying. This study allowed for detection of nanoparticles in reconstitutions that could be protein aggregates. These results also led to further studies on the optimization of formulations in order to minimize the aggregation of proteins induced by $scCO_2$ spray drying [71].

3.1.6. Fluid imaging technology

Depending on the design and flow cell characteristics, fluid imaging microscopy (also called flow imaging microscopy) measures particles in range of 1 to hundreds of μm. Flow imaging microscopy methods capture picture frames when a solution stream (containing particles) passes through a flow cell centered in the field of-view of a custom magnification system having a well characterized and extended depth-of-field. The images are analyzed to collect data with respect to count, size, concentration, as well as other aspects like shape and contrast parameters [93-95].

$ScCO_2$ spray drying processing parameters such as pressure, temperature, pressurized CO_2 and spray drying, were studied with respect to their effects on myoglobin aggregation. By fluid imaging microscopy, the formation of myoglobin aggregates was observed in the range of larger than 1 μm after the myoglobin/trehalose formulation was incubated in the pressurized CO_2 (65-130 bar and 25-50°C) without spray drying. The aggregation was explained to have been induced by CO_2 acidification as the pH of the myoglobin formulation was decreased from 6.2 to about 5 [70]. This study is among the few that raised awareness that the $scCO_2$ processing under uncontrolled conditions may destabilize proteins. In other research studies on $scCO_2$ particle formation, biodegradable particles containing biologics were successfully analyzed by flow imaging microscopy [56, 57].

3.1.7. Light obscuration (LO)

Light obscuration is the blockage of light by particles in a suspension, when particles pass through the lit pathway. Analysis of the shadow of particles allows for extracting particle size distribution and concentration. This technique is able to measure particle sizes in the range of 1-200 μm. LO is currently, besides optical microscopy, the listed technique in the US and European pharmacopeias for giving specifications of sub-visible particle concentration in parenteral solutions [96-98]. LO, however, would give an inaccurate estimation of particle sizes and concentrations where there is a low optical contrast or small difference in the refractive index of the particles and the suspending fluid [93]. Despite the attractive features, LO has not been a frequently used particle characterization method in the area of particle engineering by $scCO_2$ techniques. In the single example included in Table 1, Sathigari et al. [52] obtained the particle size distribution of antifungal itraconazole microflakes with and without additives by LO and SEM. However, the average particle size from LO was smaller than the estimated average size derived from SEM images. As shown by the

images, the itraconazole without additives had more of a rectangular shape, while the itraconazole with additives formed the spherical cluster of rectangular shape, called microflakes. This study showed that LO has limitations in analyzing non-spherical particles.

3.1.8. Scanning mobility particle sizer spectrometry (SMPS)

Scanning mobility particle sizer spectrometry (SMPS) is typically used for measuring aerosols in the range of 2.5-1000 nm [99, 100]. The particles are brought to a bipolar charger to create electrical charges on particles, which are then separated in an electrical field in a differential mobility analyzer (DMA). The separation is by means of their electrical mobility (depending on particle diameter and charge). SMPS is particularly useful for determining size of particles in a solid dosage form, which is applicable to determine particles for inhaled drugs [101] and other powdered products [100].

SMPS was integrated in a RESS setup to monitor the size of naproxen-loaded PLA particles during the expansion in an aerosol phase. The particle size distribution was obtained and related to the particle production time in the RESS process. Pure naproxen particles showed an increase in the median diameter with increasing the processing time, whereas the naproxen-PLA did not. This implied that PLA helps to reduce the agglomeration of naproxen [46]. In this case, the in situ SMPS in the RESS process assisted to determine the particle size distribution before the end of the particle preparation process.

3.1.9. Flow field-flow fractionation (Flow FFF)

Flow field-flow fractionation (flow FFF) has become an interesting analytical separation technique used as a standard method for size characterization of protein aggregates and high molecular weight polymers (>10 MDa) as well as nano- and micro-sized particles. The separation is based on variations in the diffusion coefficient, described in the Stokes-Einstein equation, as a function of diameter, temperature and viscosity of samples [47]. Many operation setups have been developed such as symmetrical and asymmetrical parallel plate flow channels [48-51], trapezoidal asymmetrical parallel plate flow FFF [52-54] and circular hollow fiber flow FFF [55]. The underlying principle of the technique, however, remains the same.

Trapezoidal asymmetrical parallel plate flow FFF is a standard commercially available asymmetrical parallel plate flow FFF (AF4) [47]. In brief, the particles are introduced into a separation chamber on the top of a membrane near the inlet of the channel flow medium. Particles

are pushed and concentrated on the membrane by means of a cross flow. The different diffusion coefficient of particles allows the small particles which diffuse back faster to be rearranged on top of the larger ones. When the secondary flow in the direction of channel is introduced, the small particle sizes will be firstly eluted at the channel outlet, followed by the larger particles due to gradient flow speed that is faster in the center and slower towards the edges of the channel.

AF4 coupling with a refractometer, UV/Vis and fluorescence spectrophotometers and a multi-angle light scattering detector allows for determining the size and concentration of particles [92]. As shown by a study of Müller et al. [102], TiO_2 nanoparticles in a sunscreen were investigated for the labelling of nanoparticle-containing consumer products with respect to the EU regulation on cosmetics and food. Before analyzing the TiO_2 nanoparticles, a $scCO_2$ extraction process was chosen instead of using a solvent extraction method to remove lipid components in a sunscreen. Using the AF4 method, the UV detector was used to determine the concentration of TiO_2 nanoparticles while the light scattering detection module gave information concerning the nanoparticle size. The results showed that the size and concentration of the TiO_2 nanoparticles in the sunscreen were comparable to that of the unformulated nanoparticles. An aggregation of TiO_2 nanoparticles was also observed by the AF4 technique. Despite its capacity, particularly the wide size range of detection, the AF4 method has not been used to characterize $scCO_2$-engineered particles.

3.1.10. Disc centrifugal sedimentation

With this technique particles are separated based on settling velocity upon a rotation of a disc centrifuge plate [103, 104]. This method is used for nanoparticle characterization. To determine the size, particles are introduced into a rotating disc, which is filled with a slight density gradient fluid for stabilization with respect to the sedimentation velocity. Upon centrifugation, particles are spun out through the fluid and detected by light attenuation. This settling velocity can be correlated to the size of the particles. The rheological properties of the fluid (density, viscosity) are calculated using polyvinyl chloride standard particles with known density and hydrodynamic diameter. This method has been shown to be able to distinguish small differences in the size of nanoparticles in a dispersion, which is quite challenging for many other techniques such as DLS[105].

3.1.11. Tunable resistive pulse sensing (TRPS)

This technique measures the mobility of individual particles. The system is composed of a tunable membrane with an orifice (a sensing zone), the two sides of which are covered with an electrolyte solution. An electrical current is applied to both sides of the electrolyte solution. When particles are introduced at one side and pass through the orifice; the electrical current of the system will be temporarily changed giving a signal of short-lived electrical impedance for each particle. The height of the signal represents the particle size, whereas the frequency of the signals is a measure of the concentration of particles. The flow of particles through the orifice is controlled by a vacuum unit. Due to the electrophoretic mobility, this technique can also perform zeta potential measurements using Smoluchowski's approximation [106, 107]. TRPS is applicable to measure submicron-sized particles, such as 100-400 nm liposomes [108], 570 nm conductive polymer microgels [109], 1 μm magnetic spheres and aggregates [110] and emulsions less than 1 μm size [106]. Although TRPS has not been used to analyze particles prepared by $scCO_2$ processes, it is may be a promising method to determine individual particles in a suspension.

3.2. Drug loading and release

Drug loading is a process to incorporate drugs into carriers, dependent on the physicochemical properties of drugs and excipients. Incorporation process is based on several mechanisms of interactions between the drugs and the carrier such as hydrogen bonding, ionic interaction, dipole interaction, physical entrapment, precipitation, covalent bonding or surface absorption [111]. Typically in order to measure the total amount of drug in the particles, drug/excipient particles are often dissolved in an aqueous medium or organic solvent and the amount of the drug in the solution is measured by using a variety of techniques that will be discussed below [112, 113].

Drug release is a reverse process of detachment of the drug from carriers, to be ready for pharmacological action. A study of drug release can provide information of drug-excipient interactions and a prediction of *in vivo* behavior [111]. By using in vitro drug release tests, the particle production process can be optimized to achieve the desired release characteristics before *in vivo* pharmacokinetic tests are performed. In addition, *in vitro* results can guide certain aspects of the design of *in vivo* studies, such as sampling times [51]. In a typical *in vitro* release study, a separation of the drug from a particle matrix is needed. Often this separation is achieved by means of dialysis. A dialysis membrane will separate particles from released drug that can diffuse through the

membrane into a release medium [114]. The release medium is collected at time intervals and analyzed by a selection of techniques that allow precise determination of the drug concentration. Use of centrifugation and filtering is also common for separation of the released drug from the particles. *In vitro* drug release is usually measured in physiological buffers at the physiological temperature (37°C) [115]. Phosphate-buffered saline (PBS), with a pH of 6.8 or 7.2, is the most commonly used dissolution buffer for $scCO_2$ engineered particles (Table 1). Simulated gastric or intestinal fluid has also been used as a dissolution medium when the purpose is oral delivery. Sometimes additional reagents such as surfactants (e.g., polysorbate 20, polysorbate 80 or sodium dodecyl sulfate) or bacteriostatic agents are added to the dissolution medium to prevent surface adsorption of the released drug or to hinder bacterial growth in long-term release experiments [116, 117].

For preparation of controlled release particles by $scCO_2$ processes, various carriers have been used such as 1-vinyl-2-pyrolidone, dextran, PLA, PLGA and PEG (Table 1). Often the drug release mechanisms are complicated, for instance, for PLGA particles drug release involves drug diffusion through water-filled pores and a polymer, osmotic pumping, and polymer erosion. A drug release mechanism could be predicted by the release profiles in the so-called phase I, II and III. In the tri-phasic profile, phase I is a burst release due to the attribution of drugs on the surface of particle, followed by a slow release profile (phase II) of drug diffusion through matrix pores with the beginning of PLGA degradation. Phase III is a second burst release after the PLGA erosion [44-46]. Drug loaded PLGA microspheres showed differences in tri-phasic release profiles of phase I, II and III, depended on particle size, morphology and drug loading [44-46, 55-57]. An example study of Porta et al. [46] prepared insulin-loaded PLGA microspheres by a double emulsion method with $scCO_2$ solvent extraction. The results showed that the size of PLGA microparticles did not influence the loading degree but had great effects on the release of insulin particularly on the first day of the experiment.

3.2.1.UV/Vis and fluorescence spectrophotometry and liquid chromatography

UV/Vis and fluorescence spectroscopy are common techniques for quantifying the drug loading in the particles and released drugs (see Table 1 and Fig. 1). Whereas UV/Vis spectroscopy is more straightforward, fluorescence spectroscopy may be a preferred choice in cases where the sensitivity of UV/Vis is not sufficient or when excipients have UV absorbance and interfere with the UV signal. For that purpose

the drug is sometimes labelled with a fluorescence tag in order to have a stronger and more selective signal. In addition, there are a variety of biochemical assays in which interaction of secondary molecules with the drug results in a color change that is detectable by UV or fluorescence signals. In another widely used approach, UV and/or fluorescence detection coupled to the liquid chromatography are employed for determination of the loading and release. Liquid chromatography allows for separation of the drug from excipients, leading to enhanced selectivity. Moreover, concentrating the drug component in chromatography technique may increase sensitivity. As seen in Table 1, the application of UV/Vis and liquid chromatography is very broad for determining various categories of drug compounds, such as proteins [69, 70, 118, 119], nonsteroidal anti-inflammatory drugs [41, 87, 120] and many others [81].

3.2.2.Thermogravimetric analysis (TGA)

Another method that has been used to study the drug loading is TGA. During a typical TGA analysis, a sample is gradually heated, while continuously being weighed, thereby measuring the weight gain/loss as function of the temperature. Mass loss may result from solvent evaporation, dehydration or degradation of the drug or excipients [121]. TGA can be used to quantify inorganic components in particles by performing the analysis up to a temperature at which drugs or other constituents are degraded. For example, in a study by Li-Hong et al. [122], where ibuprofen was loaded into silica microparticles with the assistance of $scCO_2$, the TGA curve associated with ibuprofen evaporation was found at an elevated temperature (150-250 °C) in the loaded silica microparticles. This study allowed for determination of the ibuprofen loading degree in the silica particles, showing that an increase in operating pressures of the $scCO_2$ impregnation process resulted in an increase in the degree of ibuprofen loading in silica microparticles.

3.3. Structure of drug/excipient components

Particles made by $scCO_2$ are drug/excipient complexes prepared with different drug depositions or encapsulation approaches that can result in chemical and/or physical changes in the native structure of the original components. Below we discuss methods to determine the structure of drug/excipient components after particle engineering processes by $scCO_2$.

3.3.1.Differential scanning calorimetry (DSC)

DSC allows for the identification of the temperatures at which thermal transitions like melting, glass transition and degradation occur [123]. The most common use of DSC in $scCO_2$ particle characterization is to compare the thermal characteristics of particles produced with $scCO_2$ technology with those of the individual components and/or physical mixtures. The absence of a melting and/or crystallization transition in a DSC thermogram may indicate that the material is in an amorphous state. The formation of particles exhibiting a disordered structure of drug and excipient, mostly results in an apparent increase in solubility, dissolution rate and oral bioavailability [124].

Additionally, a DSC thermogram can be used to indicate the presence of a molecular interaction between certain particle constituents. In a study by Kang et al. [112], after indomethacin was loaded in a polymeric matrix by using a SED process, the glass transition temperatures of the excipients and the melting point of the drug were lower than those of the physical mixture, indicative of a molecular interaction between the drug and the polymers. In another study by Cha et al. [61], the area under the melting peak in the thermogram was used to quantify the fraction of crystalline drug (fenofibrate) in particles prepared by a melt-absorption method using $scCO_2$. In this study, some level of disorder in the final product was desired in order to promote drug dissolution rate and bioavailability. DSC could therefore be used to optimize the production process by comparing crystallinity of particles produced with different techniques and under different conditions.

3.3.2.Spectroscopic methods

3.3.2.1. Fourier-transform infrared spectroscopy (FTIR)

Infrared (IR) spectroscopy exploits the fact that certain chemical groups absorb IR light at characteristic wavelengths, depending on inter- and intramolecular interactions [125]. Comparing the FTIR spectra of the pure materials with that of a particulate formulation can confirm the presence of intended constituents in the particles. In addition, the technique can be used to show (the absence of) molecular interactions between the constituents within a particle. Peak shifts in the spectrum of the particles indicate a molecular interaction or other changes in the bond associated with the peak.

After the particle formation by a SEDS process, no molecular interactions between puerarin and PLA was found. The FTIR signals were identical to those associated with the original structure of both

components [63]. In addition, FTIR analysis supported a release study of puerarin from PLA particles by indicating that a representative peak of puerarin component completely disappeared after puerarin was released for 48 hours from microparticles [63]. Similar release studies were observed in the cases of 5-fluorouracil-SiO_2-PLA and methotrexate in multilayer PLA microspheres, obtained from SAS and SED processes [62, 64], respectively. These results suggested the physical co-precipitation of drug/excipient by the $scCO_2$ processes. In another study, a complex of fenofibrate and mesoporous silica (SBA-15) was prepared by the $scCO_2$-assisted impregnation and studied by FTIR. FTIR spectra revealed a shift in the peak associated with the silanol group of the silica constituent of the particle, which the authors ascribed to hydrogen bonding between the carbonyl group of the drug (fenofibrate) and the silanol group in the silica. This molecular interaction between drug and excipient indicated an effective loading of fenofibrate into the silica carrier [126]. In the work of Jovanović et al. [118], lysozyme formulations with and without sugar excipient were dried using a $scCO_2$ spray drying process. The structure of α-helix and intermolecular β-sheet of the reconstituted lysozyme was determined using FTIR. A decrease in the α-helix content (representing lysozyme destabilization) and an increase in the β-sheet content (indicating the formation of protein aggregates) were found in the case of lysozyme formulation without sugar. The results demonstrate the stabilizing effect of sugar on the protein during the $scCO_2$ spray drying process.

3.3.2.2. Fluorescence spectroscopy

Fluorescence spectroscopy is a light interaction technique used for the detection of fluorophores (fluorescent molecules), which absorb electromagnetic radiation with a specific energy (called the excitation wavelength) and emit the energy at a specific wavelength called the emission wavelength [127]. For protein research, tryptophan residues are often selectively excited at 295 nm, because their emission intensity and wavelength maximum are strongly dependent on their local environment, and thus can be used to probe changes in protein conformation [70, 128]. Intrinsic tryptophan fluorescence emission spectra of polyclonal IgG were similar before and after exposure of the protein to a $scCO_2$ spray drying process, suggesting that its tertiary structure was fully preserved [119]). Fluorescence spectroscopy was used to determine the heme loss of myoglobin after $scCO_2$ spray drying. Basically, the tryptophan residues in myoglobin are quenched by heme, giving a low fluorescence intensity for native myoglobin. However, the $scCO_2$ spray dried myoglobin showed an increase in the fluorescence

intensity, specifically suggesting that the heme was partially removed from myoglobin during the $scCO_2$ spray drying process [69, 70].

3.3.2.3. *Circular dichroism spectroscopy*

Another spectroscopic method is circular dichroism (CD), which is used to determine the chirality of chemical compounds, which give unequal absorption of left-handed and right-handed polarized light [129]. CD is a useful technique to determine the secondary structure of proteins in the far-UV wavelength range (190-250 nm), and the tertiary structure in the near-UV wavelength range (250-350 nm) as well as the specific binding properties of proteins (e.g., ligand binding) [69-71, 130, 131]. For a series of $scCO_2$ spray dried protein formulations based on lysozyme, a-lactalbumin, a-chymotrypsinogen A and monoclonal antibody, no changes in the Far-UV CD or Near-UV CD spectra were observed compared to the untreated formulations [71]. This suggests that there is no change in the secondary or tertiary structures of these proteins after $scCO_2$ spray drying. In a case study of myoglobin, however, the visible CD signal from the bound heme group at 409 nm was decreased after the $scCO_2$ spray drying process, while the far-UV signal of myoglobin was not altered when compared to the untreated myoglobin, suggesting that the heme binding site was altered, which could be due to the loss or dislocation of the heme group during the $scCO_2$ spray drying process [69, 70].

3.3.3.*X-ray diffraction (XRD)*

X-ray powder diffraction is used for characterization of the crystallinity in solid materials. For a crystalline material, sharp X-ray diffraction peaks will be visible, which are absent in an amorphous material. This technique has been used for $scCO_2$ particle characterization. The absence of sharp peaks observed in the spectrum of the particles indicated absence of the crystalline state in the nilotinib (tyrosine kinase inhibitor)/hydroxypropyl methylcellulose hybrid nanoparticles prepared by the $scCO_2$ anti-solvent process. The amorphous structure was shown to lead to an improvement in several properties such as desired dissolution rate of nilotinib, improved GI absorption and bioavailability in male beagle dogs [132]. XRD was also used to study the crystallinity of sugar excipients in a $scCO_2$ spray dried protein formulation. Immediately after spray drying, the X-ray diffraction peaks of sucrose were absent, but were later detected after 1 month storage at 4 °C [118]. The presence of a crystalline state is in many cases undesirable, as it can be an indication that the drug and other excipients are not molecularly dispersed. Presence of crystalline structure in the drug or excipients may suggest that the drug is locally

deposited on the surface of microparticles (rather than being mixed). For example, the incomplete encapsulation of 10-hydroxycamptothecin in PLA by a $scCO_2$ anti-solvent process led to appearance of clear peaks form the crystalline structure of the 10-hydroxycamptothecin [133]. In a different study, the polymorphism of the anti-inflammatory drug diflunisal was observed by XRD, after its precipitation in polyvinylpyrrolidone in a $scCO_2$ anti-solvent process. The polymorphism of diflunisal influenced its dissolution [134].

3.4. Particle surface analysis

3.4.1.Energy dispersion X-ray spectroscopy (EDX)

When a sample is irradiated with an electron beam, electrons present in the sample can be displaced from their electron shell. When this 'vacancy' in the electron shell is filled by an electron from a higher energy electron shell, X-rays are emitted to release excess energy. The energy of these X-rays is characteristic for the element from which they are emitted, which is exploited in the EDX to investigate the elemental composition of a sample [135].

By combining this technique with SEM, a presence of a discriminating element (that is present in one particle constituent, but not in others) can be visualized within the SEM/EDX image. In several studies this method has been used to investigate the distribution of the drug within particles, or to confirm that drug/polymer particles were produced. In a study by Kalani et al. [13], the absence of chlorine in a final product confirmed the successful elimination of the chlorinated solvent used during SAS process. Della Porta et al. [41, 45] showed the distribution of piroxicam or diclophenac sodium on a PLGA matrix after $scCO_2$ processes, by analyzing the distribution of the sulfur atom of piroxicam and the chlorine atom of diclophenac sodium. The SEM/EDX images showed low intensity of fenofibrate's chloride atom when fenofibrate was successfully impregnated in mesoporous silica using the $scCO_2$ loading process, compared to its physical mixture [136]. A similar result was found when fenofibrate was distributed into the pores of Neusilin® UFL2 (magnesium aluminometasilicate) [61]. Moreover, the group of Compardelli et al. [137] coupled EDX analysis to TEM to analyze hollow gold nanoparticles (HGNs) in PLA nanospheres, which were used to encapsulate rhodamine using a non-solvent CO_2 process. The EDX spectrum presented the composition of gold (the Au peak), and also the residual impurity of cobalt and chlorine from the synthesis of HGNs.

3.4.2. X-ray photoelectron spectroscopy (XPS)

XPS is used to measure the elemental composition of the particle surface. The technique is comparable to EDX, but the sample irradiation occurs with X-rays instead of an electron beam. In XPS, the electrons displaced by the X-rays (photoelectrons) are detected. The energy of the photoelectrons are characteristic for the elements emitting them and the number of photoelectrons emitted is directly proportional to the abundance of an element [138]. The biggest difference between the application of EDX and XPS is that XPS measures the elemental composition of the particle surface at its outermost layer up to tens of nm in depth whereas EDX provides elemental information from a depth of hundreds of nm to a couple of µm. The chance that photoelectrons escape the sample decreases exponentially with increasing depth. XPS was used by Montes et al. [139] to demonstrate that a shell was actually in place in particles that had a core-shell structure. In this study, using a SAS process to encapsulate amoxicillin in ethyl cellulose particles, UV/Vis spectrophotometry gave about 35-50% loading efficiency of amoxicillin. However, the photoelectrons emission of the nitrogen atom in amoxicillin was not found on the particle surface by XPS, suggesting that the amoxicillin was located in the core surrounded by the ethyl cellulose shell. In a study by Chen et al. [87], XPS was used to investigate the localization of Fe_3O_4 nanoparticles within PLA-magnetic microparticles, which were prepared using the Suspension-Enhanced Dispersion by supercritical CO_2 (SpEDS) process. The authors concluded that the nanoparticles were successfully encapsulated inside the microparticles, rather than adhering to the surface.

3.4.3. Atomic force microscopy (AFM)

AFM is used for studying the topography of a particle surface. AFM analysis is based on the interaction force between a tiny tip (usually made from silica or silicon nitride) on a cantilever and the sample when the tip is dragged on a sample surface. The interaction results in the deflection of the cantilever that is reflecting a laser light to a photo diode detector. The deflection data is therefore recorded and turned into a constructed image on the operating computer during measuring. AFM is mostly used to create high-resolution images in the nano-scale range [140]. The drug loading in particles may change a particle surface as found in a study of Della Porta et al. [45] where they studied the surface roughness of drug/PLGA microsphere particles produced by a $scCO_2$ technique and an emulsion method. The surface of drug/PLGA particles from both preparation methods was moderately wrinkled,

whereas that of the pure PLGA particles was smooth, indicating that the wrinkles on particle's surface may be related to the drug dispersion in the PLGA polymer.

3.5. Porosity analysis

3.5.1. Brunauer-Emmett-Teller (BET) surface area analysis and Barrett-Joyner-Halenda (BJH) pore size and volume analysis

In pharmaceutics, a porous drug carrier such as mesoporous silica and magnesium aluminometasilicate, provides a high surface area to increase drug loading capacity [61, 141, 142]. Porous particles are characterized in terms of surface area and porosity analysis before loading drugs in order to check pore availability. After filling with drugs, the surface area and porosity of the particles are normally decreased. The analysis of gas adsorption is a widely used characterization technique for porous materials [143]. The measurement is commonly conducted at -196 °C, the gas molecules (typically N_2) are allowed to absorb as a monolayer on the free surface of the particles. A rise in pressure leads to complete gas filling into pores. Changes pressure and analysis of the adsorption phenomena can be used to calculate the surface area and pore size and volume distributions by using theoretical equations by Brunauer-Emmett-Teller (BET) and Barrett-Joyner-Halenda (BJH), respectively [144, 145]. However, the gas absorption would be influenced by a heterogeneous surface of the particles [143].

Neusilin UFL2 is a fine porous powder of magnesium aluminometasilicate used for drug absorption. Cha et al. [61] used the above-mentioned method to analyze the surface area and pore size distribution of Neusilin UFL2 excipients. The specific surface area and total pore volume of Neusilin UFL2 decreased with an increasing fenofibrate-to-Neusilin UFL2 ratio. As compared to hot-melt adsorption and solvent evaporation methods, the supercritical CO_2 method facilitated complete pore filling of fenofibrate into the pores of Neusilin UFL2. Similar results were obtained by Ahern et al. [136] and Li-hong et al. [122] who reported a reduction of the pore volumes of silica microspheres after drug loading processes with $scCO_2$.

3.5.2. High-pressure mercury intrusion porosimetry (HPMIP)

In a typical intrusion porosimetry, a non-wetting liquid is intruded into a porous material at high pressure. Mercury is the most commonly used substance for this application due to its non-wetting properties on solid surfaces. An external pressure is used to force mercury into the

pores, to overcome the surface tension of the liquid and the angle of contact with the solid surface. The employed pressure and volume of mercury after intrusion and extrusion is used to determine the pore size and volume network, pore size distribution, density and particle size. [146]. This technique can be applied for pore sizes between 3.5 nm and 500 μm [146]. For HPMIP to be effective, the pore structure needs to be accessible via the surface of the particle, and also interconnected. Usually HPMIP shows smaller pore sizes compared with SEM or optical micrographs [146].

In recent studies [66, 67], solid microspheres of lysozyme/PLA with ammonium bicarbonate (used to make pores) were formed by the PCA process. In order to obtain porous microparticles, the ammonium bicarbonate was eliminated in a vacuum step and HPMIP and SEM were used to determine the porosity of particles, which was then used to evaluate their potential aerodynamic behavior. The result showed that an increase in particle porosity led to a decrease in a density of particles, which in turn influenced the aerodynamic behaviour [66, 67].

3.6. Surface charge

The zeta potential is a measure of the surface charge of particles in a suspension [147]. More specifically, it is the average electrostatic potential between the slipping plane of a particle and a point in the fluid phase (away from the particle) [148]. Zeta potential is not measured directly, but theoretical models are used to calculate it [149].

Zeta potential is often used to predict the colloidal stability of drug-loaded particles produced by $scCO_2$ processes [91, 132, 150]. A large absolute zeta potential will result in repulsion between particles, which increases the colloidal stability of suspensions by reducing agglomeration [151]. Absolute zeta potentials above 30 mV are generally required for sufficient electrostatic stabilization, although steric stabilization can supplement a relatively low electrostatic stabilization. The zeta potential was used as an indicator to evaluate incorporation of positively-charged lysozyme in negatively-charged $CaCO_3$ particles during a $scCO_2$ process. The results showed that the negative zeta potential of $CaCO_3$ particles was decreased when lysozyme was incorporated into the particles [152].

A particle's zeta potential also may affect its pharmacokinetics, mucoadhesion and toxicity, but these aspects have not been addressed in studies dealing with $scCO_2$ engineered particles presented in Table 1. Zeta potential has been manipulated to achieve a desired targeting or biodistribution. Chitosan, a deacetylated derivative from a

naturally occurring polysaccharide, can be used to produce particles with a positive zeta potential [153]. This positive charge gives the particles mucoadhesive properties where the negative charge of the mucus and mucosal surface promote electrostatic interaction with the particles [153, 154]. Zeta potential has also been reported to affect protein adsorption; for instance, positive zeta potentials result in more adsorption of bovine serum albumin, which has a negative zeta potential at pH 7.4 [9, 155, 156]. The cytotoxicity of nanoparticles has also been related to their surface charge; positively charged particles tend to be more cytotoxic in non-phagocytic cells and could cause membrane damage. Negatively charged particles are more likely to cause intracellular damage and apoptosis [157].

3.7. Biotherapeutic activity and efficacy

A major goal in clinical pharmacology is to understand the dose-effect of designed drugs on biotherapeutic efficacy. The intrinsic activity has to do with the determination of biological responses regarding to an affinity of drug binding to a receptor, while the potency is related to the amount of drug required to give a therapeutic effect. For drug delivery applications, it has been suggested that particle formation by $scCO_2$ processes can improve biotherapeutic efficacy, drug targeting or reduce drug toxicity. However, as shown in this review paper, most of the studies so far are mainly focused on optimizing conditions for the preparation of drug/excipient nano- and microparticles for an application and only a limited number of studies go beyond particle preparation. The testing of drug activities in these papers are mostly carried out by *in vitro* methods that are related to the original activities of model drugs such as enzyme activity [66, 152], antioxidant property [158], antibacterial activity [76] and cell culture based assays (e.g., cell proliferation and antitumor activity) [91, 112] [67]. In addition, a few cited articles show that nano- and microparticles engineered by $scCO_2$ technology are applicable to vaccine and therapeutic protein delivery. For these specific applications, animal models (e.g., rats, rabbits and monkeys) are used to observe drug bioavailability after intravenous, oral, subcutaneous, and pulmonary administration. Drug levels and therapeutic efficacy in biological systems are usually determined by withdrawing blood serum from the animals [55, 65]. Particle based formulations often show improved biotherapeutic efficacy and bioavailability with the effect of a sustained drug release. For instance, a single shot tetanus toxoid/PLGA microparticles from the PGSS (NanoMix™) process was able to maintain the antigen activity for five months and potentially repeat the stimulation of antigen presenting cells that, in turn, could lead to the elimination of the need for booster

dosage of the vaccine [55]. In another example, 5-fluorouracil-loaded PLA-PEG/PEG nanoparticles prepared using the reverse emulsion-SEDS process showed a prolonged drug release and half-life, as well as an increase in diffusion into a tumor tissue. Compared to the non-particulate 5-fluorouracil, the nanoparticles improved an inhibition rate on tumor cells and increased the lifespan by a factor two [65].

3.8. Toxicology

In vitro experiments are important for the initial toxicological studies of micro/nanoparticles because they can provide mechanistic information and are inexpensive compared to animal studies [159, 160]. There are several *in vitro* assays for cytotoxicity, which can measure cell viability or test for a certain mechanism of toxicity [161]. Cell viability assays evaluate toxicity of particles by monitoring processes like membrane integrity, metabolic activity and DNA synthesis. Mechanistic assays monitor specific types of toxicity, such as DNA damage or oxidative stress. However, the absorption/emission spectra and light scattering of nanoparticles can in some cases result in false positive/negative signals in colorimetric assays [159]. In other cases particles interfere with the assay though unintended chemical reactions with reagents; for instance, several types of particles have been shown to interfere with the MTT assay, by reducing the tetrazolium salt to the product, resulting in a reported cell viability of over 100% [161]. Therefore, it is important to confirm absence of interference of a particle with the *in vitro* toxicology assay in order to ensure that the results are valid [162].

Zhang et al. [65] observed an *in vivo* hepatotoxicity on rats after administering 5-fluorouracil-loaded PLA-PEG/PEG nanoparticles prepared by a reverse emulsion-SEDS process. The liver cells stained with haemotoxylin and eosin dyes were investigated by using electron microscopy. The nanoparticles from the $scCO_2$ process showed no harmful drug hepatotoxicity on rats comparable to the untreated group.

3.9. Residual solvent and water content analysis

Organic solvents are occasionally used in $scCO_2$ particle engineering techniques or during preparation of emulsion samples. Residual solvents in the final product may cause toxicity and therefore certain limits for residuals in the pharmaceuticals have been proposed by the ICH harmonized guideline Q3C (R5) [101]. Residual organic solvents can be analyzed by the static head-space method of gas chromatography (GC). The sample is incubated at relative high temperature to allow the evaporation of solvents as a gas phase, which will be separated in a stationary column. Generally speaking $scCO_2$

techniques usually help to remove residual organic solvents because of solubility of organic solvents in $scCO_2$. After the depressurization process, the solvent concentration in particle products is often less than other conventional encapsulation methods [18, 21, 33, 81, 102].

The residual water content of dried particles has been shown to influence the stability of the particles and also that of incorporated biopharmaceuticals during storage. [71, 163] A common method to determine the residual water content is Karl Fischer titration [71]. Alternatively, TGA can be used to determine the amount of residual moisture and/or solvent in a sample by monitoring the weight loss when the sample is heated. For example, TGA coupled with FTIR was used by Bouchard et al. [164] in order to determine the amount of residual water and ethanol in $scCO_2$ dried protein formulations.

3.10. Other specific properties

The particle characterization techniques described above may not be exhaustive and other characterization techniques may be needed, depending on the type or the functionality of particles. An example of a drug delivery functionality is mucoadhesion, which can be desired if the target tissue is one with a mucosal surface, such as targets in respiratory and gastrointestinal systems [165], or when systemic effects following mucosal administration are the aim [166]. In a study by Patel et al. [113], an *ex vivo* wash off test was performed after applying microparticles to a piece of rat stomach mucosa. This allowed the authors to evaluate mucoadhesion, prior to any *in vivo* experiments.

Another example of particles that require additional characterization are magnetic particles. Magnetic particles can be used as an MRI contrasting agent, but could also be guided to the target tissue with a magnetic field [167]. In two $scCO_2$ particle engineering studies, particles were created containing Fe_3O_4, a drug and a polymer [87, 90]. The saturation magnetization of the particles was measured by a vibrating sample magnetometer, to confirm that particles with desirable magnetic properties were successfully created.

4. Summarizing discussion

The analysis of the information gathered in this review (Fig. 1) indicates that when particle products are obtained, normally, particle size and morphology are investigated as key properties that points to the success of the particle preparation process [11]. Concerning this class of properties, it is noteworthy that, often, a single characterization method

is unable to provide a full picture with respect to the size and morphology. For instance, although light scattering methods such as dynamic light scattering (DLS) and laser diffraction (LD) are often chosen to obtain information about particle size and size distribution, these methods have serious shortcomings especially when the analyzed sample has a wide size distribution [92]. Moreover, DLS and LD do not give information about the number of particles. In addition, the particle size is usually presented in the form of an average diameter, however, many particles are produced in asymmetric shapes with different ratios of horizontal and vertical projections. Shape factor often causes considerable disagreements between measured average diameter and real size for a range of particle size analyzers. As a result, to improve the reliability of particle size determination, it would be recommendable to use a couple of techniques that use different physical principles (so called orthogonal methods), such that method specific limitations do not compromise the overall picture [168]. In this context it is recommendable to use one of the imaging-based techniques, to give information about the size, shape and other general aspects at the same time [8].

Furthermore, the drug loading degree and *in vitro* drug release are among the most studied parameters that help understanding the quantity and quality of drug incorporation in a particulate system. However, it is important to realize, that the other properties may be determining parameters for pharmaceutically relevant particles, particularly because the $scCO_2$ processes may change the structure of drugs and carriers. For instance, Keles et al. [169] found that $scCO_2$ enhanced the hydrolysis of PLGA (that was used as a matrix carrier for the drug), thereby creating a porous structure when the ratio of lactide to glycolide was low. Similarly, the particle formation process may also lead to the degradation of active ingredients, such as protein drugs that have been shown to undergo destabilization by CO_2 acidification [70]. Other processing parameters in $scCO_2$ technologies may also cause degradation (e.g., structural change, loss of activity and aggregation) of proteins.

Therefore, analysis of the drug/excipient structure is the next widely studied category of properties in particles prepared with $scCO_2$ technologies. Considering the susceptibility of biopharmaceuticals to degradation and also the fast growth of this group of drugs in modern medicine, special consideration regarding the characterization of particles that carry these drugs will be underway. A number of studies have used analytical techniques (such as UV/Vis spectroscopy, circular dichroism, fluorescence spectroscopy, size-exclusion chromatography and flow-imaging microscopy) for mere purpose of characterization of

protein structure and aggregation [70, 71]. These tools were also able to characterize typical $scCO_2$ dried proteins such as lysozyme, a-lactalbumin, a-chymotrypsinogen A, monoclonal antibody and myoglobin [70, 71]. Considering that it is difficult to recommend a set of standard analytical techniques for determining protein integrity due to the diversity and specificity of each protein as well as the type of particles, the selection of techniques is based on the product of interest. Numerous fundamental techniques for characterization of therapeutic proteins are summarized and explained elsewhere [170, 171].

Following these principal properties, surface chemistry of the particles as well as surface charge are among the ones that have been addressed in the $scCO_2$ literature. Some important properties such as porosity of particles, pharmacological activity and cytotoxicity are also studied although less frequently. Some other parameters such as storage stability of the $scCO_2$-engineered particles have not been addressed despite the fact that insufficient stability can hinder the applicability of particles for drug delivery applications [172].

Observed differences in the frequency of use of particle characterization techniques are in principle related to how basic the properties are and for what purpose they are prepared. We cannot rule out the possibility that it may also depend on less scientific factors such as the straightforwardness of a certain characterization or availability of equipment in the workplaces. In addition, availability of knowledge concerning the relations between a certain property and function would result in an incentive for in-depth characterization in that area. For instance, recent knowledge concerning the stability issues associated with biopharmaceuticals has led to extra attention to the use of methods that address those. Overall, establishment of a good scientific ground for preparation of particles with desired size and loading properties would make room for more thorough characterization with respect to other potentially relevant properties such as bioactivity, toxicology, clinical trials and long-term particle stability.

Table 2. Particle characterization techniques used and potentially useful in $scCO_2$ technologies for particle engineering.

Particle characterization technique	Principle	Applicability limits and other considerations
1. Particle size distribution and morphology		
Dynamic light scattering (DLS)*	Relates the variation of the light scattering signal coming from particles in a suspension to their Brownian motion and size (random particle movements are related to particle size, viscosity, and temperature)	For particles in the range of 5-1000 nm, For liquid samples and particles in a suspension, Difficult to analyze polydisperse samples, No concentration information, No shape information
Laser diffraction (LD)*	Analysis of the scattering of static light by particles in a suspension at multiple angles	For particles in the submicron to millimetre size range, Liquid sample, Requires large amount of sample, No concentration information, No shape information
Scanning electron microscopy (SEM)*	Electron beam interacts with the surface and backscattered or secondary electrons coming out of the surface is detected. This information is used to reconstruct an image	For particles in the range of a few nm up to a hundreds of µm, For dried particles, Low throughput analysis, Needs sample treatment such as applying a conductive coating, No information about concentration, Very informative about the shape and features of the particles

Transmission electron microscopy (TEM)*	Electron beam interacts with the thin sample and electrons coming out of the other side of the thin sample are detected. This information is used to reconstruct an image	for particles in the range of a few nm up to a hundreds of µm, For dried particles, Low throughput analysis, No information about concentration, Very informative about the shape and features of the particles
Optical microscopy (OM)*	Magnification by use of an object and an eye lens	For particles in the range of a µm to hundreds of µm, Suitable for both liquid and dry samples, Low throughput analysis, No information about concentration, Very informative about the shape and features of the particles
Nanoparticle tracking analysis (NTA)*	Tracking of light scattering signal coming from individual particles in a suspension and relating the movement of particles to the size	For particles in the range of 20-1000 nm, For liquid samples and particle in a suspension, Multiple parameter settings during video recording and particle analysis, Provides concentration information, No shape information
Fluid imaging microscopy*	Particle suspension flowed in a narrow chamber and imaged	For particles in the range of a µm to hundreds of µm, Liquid sample, Provides concentration information, Very informative about the shape and features of the particles

Light obscuration (LO)*	Blocking of light by particles in a suspension and analysis of the shadow to get information about the size	For particles in the range of a µm to hundreds of µm, Liquid sample, Provides concentration information, Sensitive to presence of translucent particles, No shape information
Scanning mobility particle sizer spectroscopy (SMPS)*	Particles charged and their mobility analyzed and related to the size	For particles in the range of 2-1000 nm, For dry particles, No shape information
Flow field-flow fractionation (Flow FFF)	Separation of particles in a flow channel as a result of size dependent diffusion properties	For particles in the range of nm to a few µm, For liquid samples, Optimization for each sample required, No shape information
Disc centrifugal sedimentation	Analysis of the sedimentation velocity of particles under centrifugation	For particles in the range of a few nm to hundreds of nm, Liquid sample, Need for optimization of the fluid density gradient, Size determination depending on calibration particles, No direct concentration information
Tunable resistive pulse sensing (TRPS)	Particles passing a narrow pore influence the baseline electrical resistance between the two sides. This resistance is proportional to the size of particles	For particles in the nm size range or µm size range depending on the type of membranes and the pore size, Liquid sample, Baseline signal is sensitive to small changes

		in the environment and is difficult to stabilize
2. Drug loading and release		
UV/Vis and fluorescence spectroscopy*	Analysis of the interaction of light with the drug at a certain wavelength in the UV/Vis range and relating it to the concentration of the drug	Straightforward and reliable for determining the concentration of drugs, Liquid sample, The detection limit may be relatively high for some samples, Interference by scattered light from particles/separation needed
Chromatography tools* (e.g. liquid chromatography)	Separation of the drug in a column and measuring the concentration of it using a range of detectors such as UV and fluorescence detectors	Suitable for concentration measurements, Liquid sample, Allowing for detection of relatively smaller amounts due to concentrating and purifying in the separation phase, Provides information about other separated components, Separation phase and elution medium have to optimized, Sensitive to blockage of columns
Thermogravimetric analysis*	Follows the degradation of components when temperature is increased and relates it to their amount	Suitable for measuring the amount of components and carriers Depending on their reaction to heating, Dry sample
3. Structure of drug/excipient components		
Differential scanning calorimetry (DSC)*	Thermoanalytical technique for monitoring thermal events during	Suitable for obtaining information on sample crystallinity, glass transition temperature, melting point,

	heating to detect the changes in material phases	liquid and dry samples, Needs background info about the behavior of the individual components
Spectroscopic methods; - Fourier transform infrared spectroscopy (FTIR)*	Follows absorption of infrared light and relates it to the vibration status of certain chemical groups	Provides information about the chemical groups and their interaction with their environment, For dry or liquid sample, Needs sample preparation, Allows for protein structure analysis, No quantitative analysis
- Fluorescence spectroscopy*	Absorption and emission of the specific wavelength of light	Fluorophores, Liquid sample with an adequate concentration, Should know the maximum absorption and emission of light for the given fluorophore
- Circular dichroism (CD)*	Unequal absorption of left-handed and right-handed polarized light of a chiral compound. The sinusoidal wave is as a result of such two different signals of the polarized light.	Chiral compounds, Determining protein secondary and tertiary structures and specific binding property of proteins, Liquid sample should be freshly prepared, Known concentration and cuvette size are needed for the calculation of the CD signal
X-ray diffraction*	Diffraction patterns of X-ray interacting with the material analyzed and related to the order of atoms in the material	Suitable for analysis of sample crystallinity, For dry sample, Allows for determination of percentage

		crystallinity, Requires vast background knowledge on the diffraction patterns of potential components
4. Surface chemistry		
Energy dispersion X-ray spectroscopy (EDX)*	Irradiation of samples with an electron beam results in emission of X-ray due to jump of electrons from one energy band to another, the energy of these X-rays is characteristic for the element from which they are emitted	Suitable for elemental analysis at the surface of the material, For dry sample just as used for SEM, The signal is from a depth of a few hundred nm to a couple of µm, Allows for mapping of the elements on the surface, Not sensitive for light elements
X-ray photoelectron spectroscopy (XPS)*	Irradiating samples with X-ray and analysis of photoelectrons emitted from the surface, the amount and energy of the electrons give information about the abundance and type of the elements	Suitable for chemical analysis of the surface, Dry sample, Information form the outermost layer of the surface (depth of 0 – 10 nm)
Atomic force microscopy (AFM)*	Scanning of the surface of the sample with a fine tip and following the movements of the tip due to the feeling of the topographical features of the surface	Suitable for analysis of the surface topography, For solid surfaces either dry or fixed in situ, Provides a topographical map at the nanoscale, Can give information about the type of material in phase mode, Particularly suitable for composites
5. Porosity analysis		

Brunauer-Emmett-Teller (BET) Surface Area Analysis and Barrett-Joyner-Halenda (BJH) determination*	Analysis of gas pressure and gas adsorption to the surfaces of the pores, relating them to the total surface area and therewith amount and characteristics of the pores	Suitable for determination of the porosity of samples, Sample has to be dry, Particle agglomeration may lead to false impressions, Sensitive to modelling errors
High-pressure mercury intrusion porosimeter (HPMIP) *	Insertion of mercury into a porous material by pressure	Suitable for determination of pore diameter, pore volume and pore distribution, Dry sample, Not suitable for closed pores, Toxic mercury waste
6. Surface charge		
Zeta potential measurement (ZP)*	analysis of electrophoretic mobility (laser Doppler electrophoresis) of particles in a suspension	Measurement of zeta potential, Liquid sample, Zeta potential depends on pH and ionic strength of the buffer used
7. Biotherapeutic activity and efficacy		
In vitro activity assay*	Depending on the active compound, e.g., analysis of enzyme activity, antibacterial assay, antitumor activity, antioxidative activity	Difficult to model the physiological environment, Potential interference of excipients with the assays
In vivo study*	Testing of the drug delivery system in animal models; e.g., subcutaneous, IV, oral administration	Can observe bioavailability, pharmacokinetic study, biodistribution, efficacy, Complex animal model development, Expensive and laborious, May not correlate with human data

8. Toxicology		
In vitro cell-based assays*	Drug toxicity to cells; i.e., tumor cells, immune cells, fibroblast and other cells	Difficult to model the physiological environment, Potential interference of excipients with the assays
In vivo animal studies*	Drug toxicity evaluated in animal models	Expensive and laborious, May not correlate with human data
9. Residual solvent and water content analysis		
Gas chromatography (GC)*	Solvent evaporation and separation monitored	Measurement of residual solvent content, Liquid or dry samples, Challenges for less volatile substances
Karl Fischer titration*	The amount of residual water content in dry samples by titration of other compounds and colorimetric or volumetric detection of reactions	Suitable for determination of the residual water content in in dried particles
10. Other specific properties		
Mucoadhesion*	The adhesion of a material on mucosal surface studied by a range of in vitro procedures	Suitable for studying interaction of particles with mucus, Difficult to model the mucus
Magnetic measurement*	Analysis of the behavior of particles in a magnetic field	Suitable for analysis of targeting with an external magnetic field, Magnetic particles are normally good contrast agents for imaging

*Used in $scCO_2$ particle engineering

Abbreviations of $scCO_2$ engineering processes

Supercritical carbon dioxide (supercritical CO_2 or $scCO_2$)

Rapid Expansion of Supercritical Solutions (RESS)

Non-solvent RESS process (RESS-N)

Supercritical solution into a liquid solvent (RESOLV)

Aerosol Solvent Extraction System (ASES)

Supercritical Fluid Emulsion Extraction (SFEE)

Supercritical Anti-Solvent (SAS)

Precipitation with Compressed Anti-solvent (PCA)

Supercritical Anti-Solvent with Enhanced Mass Transfer (SAS-EM)

Supercritical Anti-Solvent Drug-Excipient Mixing (SAS-DEM)

Particles from Gas Saturated Solutions (PGSS)

Gas-Assisted Melting Atomization (GAMA)

Solution-Enhanced Dispersion by $ScCO_2$ (SEDS)

Suspension Enhanced Dispersion by $scCO_2$ (SpEDS)

Reverse-emulsion-Solution Enhanced Dispersion by $scCO_2$ (reverse emulsion-SEDS)

$ScCO_2$ assisted atomization (SAA)

Carbon dioxide-assisted nebulization with a bubble dryer (CAN-BD)

References

[1] O. C. Farokhzad, R. Langer, Impact of nanotechnology on drug delivery, ACS Nano, 3 (2009) 16-20.

[2] A.H. Chow, H.H. Tong, P. Chattopadhyay, B.Y. Shekunov, Particle engineering for pulmonary drug delivery, Pharm Res, 24 (2007) 411-37.

[3] M. Manzano, V. Aina, C.O. Areán, F. Balas, V. Cauda, M. Colilla, M.R. Delgado, M. Vallet-Regí, Studies on MCM-41 mesoporous silica for drug delivery: Effect on particle morphology and amine functionalization, Chem Eng J, 137 (2008) 30-37.

[4] M.L. Etheridge, S.A. Campbell, A.G. Erdman, C.L. Haynes, S.M. Wolf, J. McCullough, The big picture on nanomedicine: the state of investigational and approved nanomedicine products. Nanomedicine, 9 (2013) 1-14.

[5] A. L. Vasilakes, T.D. Dziubla, P.P. Wattamwar, Polymeric Nanoparticles. In Engineering Polymer Systems for Improved Drug Delivery, R.A. Bader and D.A. Putnam, Editors. 2014, John Wiley & Sons. p. 117-148.

[6] S.P. Schwendeman, R.B. Shah, B.A. Bailey, A.S. Schwendeman, Injectable controlled release depots for large molecules. J Control Release, 190 (2014) 240-53.

[7] P. York, U.B. Kompella, B.Y. Shekunov, Supercritical Fluid Technology for Product Development. Vol. 138. 2004, New York: CRC Press.

[8] M. Gaumet, A. Vargas, R. Gurny, F. Delie, Nanoparticles for drug delivery: The need for precision in reporting particle size parameters, Eur J Pharm Biopharm, 69 (2008) 1-9.

[9] F. Alexis, E. Pridgen, L.K. Molnar, O.C. Farokhzad, Factors affecting the clearance and biodistribution of polymeric nanoparticles, Mol Pharm, 5 (2008) 505-515.

[10] Greish, K., Enhanced permeability and retention of macromolecular drugs in solid tumors: a royal gate for targeted anticancer nanomedicines, J Drug Target, 15 (2007) 457-64.

[11] B. Slutter, W. Jiskoot, Sizing the optimal dimensions of a vaccine delivery system: a particulate matter, Expert Opin Drug Deliv, 13 (2016) 167-70.

[12] N. Benne, J. van Duijn, J. Kuiper, W. Jiskoot, B. Slütter, Orchestrating immune responses: How size, shape and rigidity affect the immunogenicity of particulate vaccines. J Controll Release, 234 (2016) 124-34.

[13] M. Kalani, R. Yunus, Effect of supercritical fluid density on nanoencapsulated drug particle size using the supercritical antisolvent method, Int J Nanomedicine, 7 (2012) 2165-72.

[14] B.B. Kale, N.H. Aloorkar, S.M. Deshmukh, S.P. Sulake, P.V. Humbe, P.P. Mane, Recent advancements in prticle engineering techniques for pharmaceutical applications, Indo Am J Pharm Res, 4 (2014) 2027-49.

[15] R.T.Y. Lim, W.K. Ng, E. Widjaja, R.B.H. Tan, Comparison of the physical stability and physicochemical properties of amorphous indomethacin prepared by co-milling and supercritical anti-solvent co-precipitation, J Supercrit Fluids, 79 (2013) 186-201.

[16] M. Tabbakhian, F. Hasanzadeh, N. Tavakoli, Z. Jamshidian, Dissolution enhancement of glibenclamide by solid dispersion: solvent evaporation versus a supercritical fluid-based solvent -antisolvent technique, Res Pharm Sci, 9 (2014) 337-50.

[17] Z. S. Yu, K. P. Johnston, R. O. Williams, Spray freezing into liquid versus spray-freeze drying: Influence of atomization on protein aggregation and biological activity, Eur J Pharm Sci, 27 (2006) 9-18.

[18] S.D. Webb, S.L. Golledge, J.L. Cleland, J.F. Carpenter, T.W. Randolph, Surface adsorption of recombinant human interferon-gamma in lyophilized and spray-lyophilized formulations, J Pharm Sci, 91 (2002) 1474-87.

[19] M. Dissanayake, S. Liyanaarachchi, T. Vasiljevic, Functional properties of whey proteins microparticulated at low pH, J Dairy Sci, 95 (2012) 1667-79.

[20] I. Roy, M.N. Gupta, Freeze-drying of proteins: some emerging concerns, Biotechnol Appl Biochem, 39 (2004) 165-177.

[21] A. Tabernero, E.M. Martín del Valle, and M.A. Galán, Supercritical fluids for pharmaceutical particle engineering: Methods, basic fundamentals and modelling, Chem Eng Process, 60 (2012) 9-25.

[22] M. D. Louey, M. Van Oort, A.J. Hickey, Aerosol dispersion of respirable particles in narrow size distributions produced by jet-milling and spray-drying techniques, Pharmaceut Res, 21 (2004) 1200-6.

[23] T. L. Rogers, K.P. Johnston, and R.O. Williams 3rd, Solution-based particle formation of pharmaceutical powders by supercritical or compressed fluid CO_2 and cryogenic spray-freezing technologies, Drug Dev Ind Pharm, 27 (2001) 1003-15.

[24] S.A. Shoyele, S. Cawthorne, Particle engineering techniques for inhaled biopharmaceuticals, Adv Drug Deliv Rev, 58 (2006) 1009-29.

[25] E. Del Valle, M. Galan, Supercritical Fluid technique for particle engineering: Drug delivery applications, Rev Chem Eng, 21 (2005) 33-69.

[26] E. Reverchon, R. Adami, G. Caputo, I. De Marco, Spherical microparticles production by supercritical antisolvent precipitation: Interpretation of results, J Supercrit Fluids, 47 (2008) 70-84.

[27] E. Reverchon, Supercritical antisolvent precipitation of micro- and nano-particles. J Supercrit Fluids, 15 (1999) 1-21.

[28] A. Martin and M.J. Cocero, Micronization processes with supercritical fluids: fundamentals and mechanisms, Adv Drug Deliv Rev, 60 (2008) 339-50.

[29] A. Martin, and M.J. Cocero, Precipitation processes with supercritical fluids: patents review, Recent Pat Eng, 2 (2008) 9-20.

[30] N. Esfandiari, Production of micro and nano particles of pharmaceutical by supercritical carbon dioxide, J Supercrit Fluids, 100 (2015) 129-41.

[31] R. Campardelli, L. Baldino, E. Reverchon, Supercritical fluids applications in nanomedicine, J Supercrit Fluids, 101 (2015) 193-214.

[32] P. Khadka, J. Ro, H. Kim, I. Kim, J. T. Kim, H. Kim, J. M. Cho, G. Yun, J. Lee, Pharmaceutical particle technologies: An approach to improve drug solubility, dissolution and bioavailability, Asian J Pharm Sci, 9 (2014) 304–16.

[33] E. Elizondo, J. Veciana, N. Ventosa, Nanostructuring molecular materials as particles and vesicles for drug delivery, using compressed and supercritical fluids. Nanomedicine, 7 (2012) 1391-408.

[34] P.G. Debenedetti, J.W. Tom, X. Kwauk, S.-D. Yeo, Rapid expansion of supercritical solutions (RESS): fundamentals and applications, Fluid Phase Equilib, 82 (1993) 311-21.

[35] K. Matsuyama, K. Mishima, H. Umemoto, S. Yamaguchi, Environmentally benign formation of polymeric microspheres by rapid expansion of supercritical carbon dioxide solution with a nonsolvent, Environ Sci Technol, 35 (2001) 4149-55.

[36] K. Matsuyama, K. Mishima, K.-I. Hayashi, H. Ishikawa, H. Matsuyama, T. Harada, Formation of microcapsules of medicines by the rapid expansion of a supercritical solution with a nonsolvent, J Appl Polym Sci, 89 (2003) 742-52.

[37] K. Mishima, K. Matsuyama, D. Tanabe, S Yamauchi, T.J. Young, K.P. Johnston, Microencapsulation of proteins by rapid expansion of supercritical solution with a nonsolvent, Aiche Journal, 46(2000) 857-65.

[38] Y.P. Sun, M.J. Meziani, P. Pathak, L. Qu, Polymeric nanoparticles from rapid expansion of supercritical fluid solution, Chem-Euro J, 11 (2005) 1366-73.

[39] S. G. Kazarian, G.G. Martirosyan, Spectroscopy of polymer/drug formulations processed with supercritical fluids: in situ ATR-IR and Raman study of impregnation of ibuprofen into PVP, Int J Pharm, 232 (2002) 81-90.

[40] A.R. Berens, G.S. Huvard, R.W. Korsmeyer, F.W. Kunig, Application of Compressed Carbon-Dioxide in the Incorporation of Additives into Polymers, J Appl Polym Sci, 46 (1992) 231-42.

[41] G. Della Porta, E. Reverchon, Nanostructured microspheres produced by supercritical fluid extraction of emulsions. Biotechnol Bioeng, 100 (2008) 1020-33.

[42] B.Y. Shekunov, P. Chattopadhyay, J. Seitzinger, R. Huff, Nanoparticles of poorly water-soluble drugs prepared by supercritical fluid extraction of emulsions, Pharmaceut Res, 23 (2006) 196-204.

[43] P. Chattopadhyay, R. Huff, B. Shekunov, Drug encapsulation using supercritical fluid extraction of emulsions, J Pharm Sci, 95 (2006) 667-79.

[44] N .Falco, E. Reverchon, G. Della Porta, Injectable PLGA/hydrocortisone formulation produced by continuous supercritical emulsion extraction, Int J Pharm, 441 (2013) 589-97.

[45] G. Della Porta, N. Falco, E. Reverchon, NSAID drugs release from injectable microspheres produced by supercritical fluid emulsion extraction, J Pharm Sci, 99 (2010) 1484-99.

[46] G.D. Porta, N. Falco, E. Giordano, E. Reverchon, PLGA microspheres by Supercritical Emulsion Extraction: a study on insulin release in myoblast culture, J Biomater Sci Polym Ed, 24 (2013) 1831-47.

[47] M. Kalani, R. Yunus, Application of supercritical antisolvent method in drug encapsulation: a review, Int J Nanomedicine, 6 (2011) 1429-42.

[48] S. Palakodaty, P. York, Phase behavioral effects on particle formation processes using supercritical fluids. Pharmaceut Res, 16 (1999) 976-85.

[49] P. Chattopadhyay, R. Gupta, Production of griseofulvin nanoparticles using supercritical CO2 antisolvent with enhanced mass transfer, International Journal of Pharmaceutics, 228 (2001) 19-31.

[50] L. Lee, C. Wang, K. Smith, Supercritical antisolvent production of biodegradable micro- and nanoparticles for controlled delivery of paclitaxel, J Control Release, 125 (2008) 96-106.

[51] C.A. Ober, L. Kalombo, H. Swai, R. B. Gupta, Preparation of rifampicin/lactose microparticle composites by a supercritical antisolvent-drug excipient mixing technique for inhalation delivery, Powder Technol, 236 (2013) 132-38.

[52] S.K. Sathigari, C.A. Ober, G.P. Sanganwar, R.B. Gupta, R.J. Babu, Single-Step Preparation and Deagglomeration of Itraconazole Microflakes by Supercritical Antisolvent Method for Dissolution Enhancement, J Pharm Sci, 100 (2011) 2952-65.

[53] G.P. Sanganwar, S. Sathigari, R.J. Babu, R.B. Gupta, Simultaneous production and co-mixing of microparticles of nevirapine with excipients by supercritical antisolvent method for dissolution enhancement, Eur J Pharm Sci, 39 (2010) 164-74.

[54] Z. Knez, E. Weidner, Particles formation and particle design using supercritical fluids, Curr. Opin. Solid State Mater. Sci., 7 (2003) 353-61.

[55] A. Baxendale, P. van Hooff, L.G. Durrant, I. Spendlove, S.M. Howdle, H.M. Woods, M.J. Whitaker, O.R. Davies, A. Naylor, A.L. Lewis, L. Illum, Single shot tetanus vaccine manufactured by a supercritical fluid encapsulation technology, Int J Pharm, 413 (2011) 147-54.

[56] F. Jordan, A. Naylor, C.A. Kelly, S.M. Howdle, A. Lewis, L. Illum, Sustained release hGH microsphere formulation produced by a novel supercritical fluid technology: in vivo studies, J Control Release, 141 (2010) 153-60.

[57] D.R. Perinelli, G. Bonacucina, M. Cespi, A. Naylor, M. Whitaker, G.F. Palmieri, G. Giorgioni, L. Casettari, Evaluation of P(L)LA-PEG-P(L)LA as processing aid for biodegradable particles from gas saturated solutions (PGSS) process, Int J Pharm, 468 (2014) 250-7.

[58] S. Salmaso, N. Elvassore, A. Bertucco, P. Caliceti, Production of Solid Lipid Submicron Particles for Protein Delivery Using a Novel Supercritical Gas-Assisted Melting Atomization Process, J Pharm Sci, 98 (2009) 640-50.

[59] T.K. Fahim, I.S.M. Zaidul, M.R. Abu Bakar, U.M. Salim, M.B. Awang, F. Sahena, K.C.A. Jalal, K.M. Sharif, M.H. Sohrab, Particle formation and micronization using non-conventional techniques-review, Chem Eng Process, 86 (2014) 47-52.

[60] R. Dohrn, E. Bertakis, O. Behrend, E. Voutsas, D. Tassios, Melting point depression by using supercritical CO_2 for a novel melt dispersion micronization process, J Mol Liq, 131 (2007) 53-9.

[61] K.H. Cha, K.J. Cho, M.S. Kim, J.S. Kim, H.J. Park, J. Park, W. Cho, J.S. Park, S.J. Hwang, Enhancement of the dissolution rate and bioavailability of fenofibrate by a melt-adsorption method using supercritical carbon dioxide, Int J Nanomedicine, 7 (2012) 5565-75.

[62] A.Z. Chen, G.Y. Wang, S.B. Wang, L. Li, Y.G. Liu, C. Zhao, Formation of methotrexate-PLLA-PEG-PLLA composite microspheres by microencapsulation through a process of suspension-enhanced dispersion by supercritical CO_2, Int J Nanomedicine, 7 (2012) 3013-22.

[63] A.-Z. Chen, Y. Li, F.-T. Chau, T.-Y. Lau, J.-Y. Hu, Z. Zhao, D. K.-W. Mok, Microencapsulation of puerarin nanoparticles by poly(l-lactide) in a supercritical CO_2 process, Acta Biomater, 5 (2009) 2913-9.

[64] A.Z. Chen, Y. Li, D. Chen, J.Y. Hu, Development of core-shell microcapsules by a novel supercritical CO_2 process, J Mater Sci Mater Med, 20 (2009) 751-8.

[65] C. Zhang, G. Li, Y. Wang, F. Cui, J. Zhang, Q. Huang, Preparation and characterization of 5-fluorouracil-loaded PLLA-PEG/PEG nanoparticles by a novel supercritical CO_2 technique, Int J Pharm, 436 (2012) 272-81.

[66] Y.-Q. Kang, C. Zhao, A.-Z. Chen, S.-B. Wang, Y.-G. Liu, W.-G. Wu, X.-Q. Su, Study of lysozyme-loaded poly-L-lactide (PLLA) porous microparticles in a compressed CO_2 antisolvent process, Materials, 6 (2013) 3571-83.

[67] A.-Z. Chen, C. Zhao, S.-B. Wang, Y.-G. Liu, D.-L. Lin, Generation of porous poly-L-lactide microspheres by emulsion-combined precipitation with a compressed CO_2 antisolvent process, J Mater Chem B, 1 (2013) 2967-75.

[68] A. Nunes, C. Duarte, Dense CO_2 as a Solute, Co-Solute or Co-Solvent in Particle Formation Processes: A Review, Materials, 4 (2011) 2017-41.

[69] N. Jovanović, A. Bouchard, G.W. Hofland, G.J. Witkamp, D.J. Crommelin, W. Jiskoot, Distinct effects of sucrose and trehalose on protein stability during supercritical fluid drying and freeze-drying, Eur J Pharm Sci, 27 (2006) 336-45.

[70] O. Nuchuchua, H.A. Every, W. Jiskoot, Critical processing parameters of carbon dioxide spray drying for the production of dried protein formulations: A study with myoglobin, Eur J Pharm Biopharm, 103 (2016) 200-9.

[71] O. Nuchuchua, G. Hofland, H.A. Every, W. Jiskoot, Scalable organic solvent free supercritical fluid spray drying process for producing dry protein formulations, Eur J Pharm Biopharm, 88 (2014) 919-30.

[72] E. Reverchon, Supercritical-assisted atomization to produce micro- and/or nanoparticles of controlled size and distribution, Ind Eng Chem Res, 41 (2002) 2405-11.

[73] E. Reverchon, R. Adami, S. Cardea, G. D. Porta, Supercritical fluids processing of polymers for pharmaceutical and medical applications, J Supercrit Fluids, 47 (2009) 484-92.

[74] R. Sievers, Formation of aqueous small droplet aerosols assisted by supercritical carbon dioxide, Aerosol Sci Technol, 30 (1999) 3-15.

[75] S.P. Cape, J.A. Villa, E.T.S. Huang, T.-H. Yang, J.F. Carpenter, R.E. Sievers, Preparation of active proteins, vaccines and pharmaceuticals as fine powders using supercritical or near-critical fluids, Pharm Res, 25 (2008) 1967-90.

[76] R.P. Aquino, G. Auriemma, T. Mencherini, P. Russo, A. Porta, R. Adami, S. Liparoti, G. Della Porta, E. Reverchon, P. Del Gaudio, Design and production of gentamicin/dextrans microparticles by supercritical assisted atomisation for the treatment of wound bacterial infections, Int J Pharm, 440 (2013) 188-94.

[77] G. Della Porta, R. Adami, P. Del Gaudio, L. Prota, R. Aquino, E. Reverchon, Albumin/gentamicin microspheres produced by supercritical assisted atomization: optimization of size, drug loading and release, J Pharm Sci, 99 (2010) 4720-9.

[78] E. de Paz, A. Martin, M.J. Cocero, Formulation of beta-carotene with soybean lecithin by PGSS (Particles from Gas Saturated Solutions)-drying, J Supercrit Fluids, 72 (2012) 125-33.

[79] K. Schmitz, Basic Concepts of Light Scattering. In Introduction to Dynamic Light Scattering by Macromolecules, 2012, Elsevier. p. 11-42.

[80] B. J. Berne, R. Pecora, Dynamic Light Scattering: With Applications to Chemistry, Biology, and Physics. 2013, New York: Courier Dover Publications.

[81] F. Zabihi, N. Xin, S. Li, J. Jia, T. Cheng, Y. Zhao, Polymeric coating of fluidizing nano-curcumin via anti-solvent supercritical method for sustained release, J Supercrit Fluids, 89 (2014) 99-105.

[82] D. Traini, D. Traini, Inhalation drug delivery, in: P. Colombo, D. Traini, F. Buttini (Eds.), Inhalation Drug Delivery: Techniques and Products, John Wiley & Sons, Ltd., West Sussex, UK, 2013, pp. 1-10.

[83] D.A. Edwards, D. Chen, J. Wang, A. Ben-Jebria, 1998. Controlled-release inhalation aerosols. In: Respiratory drug delivery VI. Hilton Head, SC: Interpharm Press, Inc, 187-192.

[84] C.J. Musante, J.D. Schroeter, J.A. Rosati, T.M. Crowder, A.J. Hickey, T.B. Martonen, Factors affecting the deposition of inhaled porous drug particles, J Pharm Sci, 91 (2002) 1590-600.

[85] K. D. Vernon-Parry, Scanning Electron Microscopy: an introduction, III-Vs Review, 13 (2000) 40-4.

[86] A. Sane, J. Limtrakul, Formation of retinyl palmitate-loaded poly(L-lactide) nanoparticles using rapid expansion of supercritical solutions into liquid solvents (RESOLV), J Supercrit Fluids, 51 (2009) 230-37.

[87] A.Z. Chen, Y.Q. Kang, X.M. Pu, G.F. Yin, Y. Li, J.Y. Hu, Development of Fe_3O_4-poly(L-lactide) magnetic microparticles in supercritical CO_2, J Colloid Interface Sci, 330 (2009) 317-22.

[88] H. G. Merkus, in: Henk G. Merkus (Eds.), Particle Size Measurements Fundamentals, Practice, Quality, Springer Science+Business Media B.V., Netherlands, 2009, pp. 210.

[89] L. Reimer and H. Kohl, Transmission Electron Microscopy: Physics of Image Formation. 5 ed. 2008: Springer-Verlag New York Inc.

[90] A.-Z. Chen, L. Li, S.-B. Wang, X.-F. Lin, Y.-G. Liu, C. Zhao, G.-Y. Wang, Z. Zhao, Study of Fe_3O_4–PLLA–PEG–PLLA magnetic microspheres based on supercritical CO_2: Preparation, physicochemical characterization, and drug loading investigation, J Supercrit Fluids, 67 (2012) 139-48.

[91] Y. Kang, J. Wu, G. Yin, Z. Huang, X. Liao, Y. Yao, P. Ouyang, H. Wang, Q. Yang, Characterization and biological evaluation of paclitaxel-loaded poly(L-lactic acid) microparticles prepared by supercritical CO_2, Langmuir, 24 (2008) 7432-41.

[92] V. Filipe, A. Hawe, W. Jiskoot, Critical evaluation of Nanoparticle Tracking Analysis (NTA) by NanoSight for the measurement of nanoparticles and protein aggregates, Pharm Res, 27 (2010) 796-810.

[93] D.K. Sharma, D. King, P. Oma, C. Merchant, Micro-flow imaging: flow microscopy applied to sub-visible particulate analysis in protein formulations, AAPS J, 12 (2010) 455-64.

[94] D. Weinbuch, S. Zölls, M. Wiggenhorn, W. Friess, G. Winter, W. Jiskoot, A. Hawe, Micro-flow imaging and resonant mass measurement (Archimedes)--complementary methods to quantitatively differentiate protein particles and silicone oil droplets, J Pharm Sci, 102 (2013) 2152-65.

[95] S. Zölls, D. Weinbuch, M. Wiggenhorn, G. Winter, W. Friess, W. Jiskoot, A. Hawe, Flow imaging microscopy for protein particle analysis--a comparative evaluation of four different analytical instruments, AAPS J, 15 (2013) 1200-11.

[96] J.F. Carpenter, T.W. Randolph, W. Jiskoot, D.J. Crommelin, C.R. Middaugh, G. Winter, Y.X. Fan, S. Kirshner, D. Verthelyi, S. Kozlowski, K.A. Clouse, P.G. Swann, A. Rosenberg, B. Cherney, Overlooking subvisible particles in therapeutic protein products: gaps that may compromise product quality, J Pharm Sci, 98 (2009) 1201-5.

[97] S.K. Singh, N. Afonina, M. Awwad, K. Bechtold-Peters, J.T. Blue, D. Chou, M. Cromwell, H.J. Krause, H.C. Mahler, B.K. Meyer, L. Narhi, D.P. Nesta, T. Spitznagel, An industry perspective on the monitoring of subvisible particles as a quality attribute for protein therapeutics, J Pharm Sci, 99 (2010) 3302-21.

[98] A. Hawe, F. Schaubhut, R. Geidobler, M. Wiggenhorn, W. Friess, M. Rast, C. de Muynck, G. Winter, Pharmaceutical feasibility of sub-visible particle analysis in parenterals with reduced volume light obscuration methods, Eur J Pharm Biopharm, 85 (2013) 1084-7.

[99] J.G. Watson, J.C. Chow, D.A. Sodeman, D.H. Lowenthal, M.-C.O. Chang, K. Park, X. Wang, Comparison of four scanning mobility particle sizers at the Fresno Supersite, Particuology, 9 (2011) 204-9.

[100] T. Amodeo, C. Dutouquet, O.L. Bihan, M. Attoui, E. Frejafon, On-line determination of nanometric and sub-micrometric particle physicochemical characteristics using spectral imaging-aided Laser-Induced Breakdown Spectroscopy coupled with a Scanning Mobility Particle Sizer, Spectrochim Acta Part B At Spectrosc, 64 (2009) 1141-52.

[101] J. Löndahl, W. Möller, J.H. Pagels, W.G. Kreyling, E. Swietlicki, O. Schmid, Measurement techniques for respiratory tract deposition of airborne nanoparticles: a critical review, J Aerosol Med Pulm Drug Deliv, 27 (2014) 229-54.

[102] D. Müller, S. Cattaneo, F. Meier, R. Welz, T. de Vries, M. Portugal-Cohen, D.C. Antonio, C. Cascio, L. Calzolai, D. Gilliland, A. de Mello, Inverse supercritical fluid extraction as a sample preparation method for the analysis of the nanoparticle content in sunscreen agents, J Chromatogr A, 1440 (2016) 31-6.

[103] M. Nadler, T. Mahrholz, U. Riedel, C. Schilde, A. Kwade, Preparation of colloidal carbon nanotube dispersions and their characterization using a disc centrifuge, Carbon, 46 (2008) 1384-92.

[104] A. Neumann, W. Hoyer, M.W. Wolff, U. Reichl, A. Pfitzner, B. Roth, New method for density determination of nanoparticles using a CPS disc centrifuge (TM), Colloids Surf B Biointerfaces, 104 (2013) 27-31.

[105] H. Fissan, S. Ristig, H. Kaminski, C. Asbach, M. Epple, Comparison of different characterization methods for nanoparticle dispersions before and after aerosolization, Anal Methods, 6 (2014) 7324-34.

[106] J.A. Somerville, G.R. Willmott, J. Eldridge, M. Griffiths, K.M. McGrath, Size and charge characterization of a submicrometre oil-in-water emulsion using resistive pulse sensing with tunable pores, J Colloid Interface Sci, 394 (2013) 243-51.

[107] R. B. Schoch, J.Y. Han, P. Renaud, Transport phenomena in nanofluidics, Rev Mod Phys, 80 (2008) 839-83.

[108] L. Yang, M.F. Broom, I.G. Tucker, Characterization of a nanoparticulate drug delivery system using scanning ion occlusion sensing, Pharm Res, 29 (2012) 2578-86.

[109] A. Deric, Holden, G.H., L. Andrew Lyon, H. S. White, Resistive pulse analysis of microgel deformation during nanopore translocation, J Phys Chem C, 115 (2011) 2999-3004.

[110] G. R. Willmott, M. Platt, G.U. Lee, Resistive pulse sensing of magnetic beads and supraparticle structures using tunable pores, Biomicrofluidics, 6 (2012) 014103.

[111] A. Villiers, M. M. de Villiers, Drug Loading into and in vitro Release from Nanosized Drug Delivery Systems. In Nanotechnology in Drug Delivery, 2008, American Association of Pharmaceutical Scientists, pp.129-155. 40, no.

[112] Y. Kang, J. Wu, G. Yin, Z. Huang, Y. Yao, X. Liao, A. Chen, X. Pu, L. Liao, Preparation, characterization and in vitro cytotoxicity of indomethacin-loaded PLLA/PLGA microparticles using supercritical CO_2 technique, Eur J Pharm Biopharm, 70 (2008) 85-97.

[113] J. Patel, P. Patil, Preparation and characterization of amoxicillin mucoadhesive microparticles using solution-enhanced dispersion by supercritical CO_2. J Microencapsul, 29 (2012) 398-408.

[114] C. Washington, Evaluation of Non-Sink Dialysis Methods for the Measurement of Drug Release from Colloids - Effects of Drug Partition, Int J Pharm, 56 (1989) 71-74.

[115] S. S. D'Souza, P.P. DeLuca, Methods to assess in vitro drug release from injectable polymeric particulate systems, Pharm Res, 23 (2006) 460-74.

[116] E. Elizondo, S. Sala, E. Imbuluzqueta, D. González, M.J. Blanco-Prieto, C. Gamazo, N. Ventosa, J. Veciana, High loading of gentamicin in bioadhesive PVM/MA nanostructured microparticles using compressed carbon-dioxide, Pharm Res, 28 (2011) 309-21.

[117] S. Ravi, K.K. Peh, Y. Darwis, B.K. Murthy, T.R. Singh, C. Mallikarjun, Development and characterization of polymeric microspheres for controlled release protein loaded drug delivery system, Indian J Pharm Sci, 70 (2008) 303-9.

[118] N. Jovanović, A. Bouchard, M. Sutter, M. Van Speybroeck, G.W. Hofland, G.J. Witkamp, D.J. Crommelin, W. Jiskoot, Stable sugar-based protein formulations by supercritical fluid drying, Int J Pharm, 346 (2008) 102-8.

[119] N. Jovanović, A. Bouchard, G.W. Hofland, G.J. Witkamp, D.J. Crommelin, W. Jiskoot, Stabilization of IgG by supercritical fluid drying: optimization of formulation and process parameters, Eur J Pharm Biopharm, 68 (2008) 183-90.

[120] M. Gadermann, S. Kular, A.H. Al-Marzouqi, R. Signorell, Formation of naproxen-polylactic acid nanoparticles from supercritical solutions and their characterization in the aerosol phase, Phys Chem Chem Phys, 11 (2009) 7861-8.

[121] M. E. Brown, Introduction to Thermal Analysis: Techniques and Applications. 2001: Springer Science & Business Media. 264.

[122] W. Li-Hong, C. Xin, X. Hui, Z. Li-Li, H. Jing, Z. Mei-Juan, L. Jie, L. Yi, L. Jin-Wen, Z. Wei, C. Gang, A novel strategy to design sustained-release poorly water-soluble drug mesoporous silica microparticles based on supercritical fluid technique, Int J Pharm, 454 (2013) 135-42.

[123] P. Gill, T.T. Moghadam, B. Ranjbar, Differential scanning calorimetry techniques: applications in biology and nanoscience, J Biomol Tech, 21 (2010) 167-93.

[124] M. Zhang, H. Li, B. Lang, K. O'Donnell, H. Zhang, Z. Wang, Y. Dong, C. Wu, R.O. Williams 3rd, Formulation and delivery of improved amorphous fenofibrate solid dispersions prepared by thin film freezing, Eur J Pharm Biopharm, 82 (2012) 534-44.

[125] F. Rouessac, A. Rouessac, Infrared Spectroscopy, in Chemical Analysis: Modern Instrumentation Methods and Techniques. 2007, John Wiley & Sons Ltd. p. 207-40.

[126] R. J. Ahern, A. M. Crean, K. B. Ryan, The influence of supercritical carbon dioxide ($SC\text{-}CO_2$) processing conditions on drug loading and physicochemical properties, Int J Pharm, 439 (2012) 92-9.

[127] A. B. Ghisaidoobe, S.J. Chung, Intrinsic tryptophan fluorescence in the detection and analysis of proteins: a focus on Forster resonance energy transfer techniques, Int J Mol Sci, 15 (2014) 22518-38.

[128] W. Jiskoot, A. J. W. G. Visser, J. N. Herron, M. Sutter, Fluorescence spectroscopy. In: Methods for Structural Analysis of Protein Pharmaceuticals (W. Jiskoot and D.J.A. Crommelin, Eds.), AAPS Press, Arlington, VA, 2005: p. 27-82.

[129] N. J. Greenfield, Using circular dichroism spectra to estimate protein secondary structure, Nat Protoc, 6 (2006) 2876-90.

[130] A. Rodger, R. Marrington, D. Roper, S. Windsor, Circular dichroism spectroscopy for the study of protein-ligand interactions, Methods Mol Biol, 305 (2005) 343-64.

[131] M. Bloemendal, W. Jiskoot, Circular dichroism spectroscopy. In: Methods for Structural Analysis of Protein Pharmaceuticals (W. Jiskoot and D.J.A. Crommelin, Eds.). AAPS Press, Arlington, VA, 2005: p. 83-130.

[132] G. Jesson, M. Brisander, P. Andersson, M. Demirbüker, H. Derand, H. Lennernäs, M. Malmsten, Carbon dioxide-mediated generation of hybrid nanoparticles for improved bioavailability of protein kinase inhibitors, Pharm Res, 31 (2014) 694-705.

[133] W. Wang, G. Liu, J. Wu, Y. Jiang, Co-precipitation of 10-hydroxycamptothecin and poly (L-lactic acid) by supercritical CO_2 anti-solvent process using dichloromethane/ethanol co-solvent, J Supercrit Fluids, 74 (2013) 137-44.

[134] F. Zahran, A. Cabañas, J.A.R. Cheda, J.A.R. Renuncio, C. Pando, Dissolution rate enhancement of the anti-inflammatory drug diflunisal by coprecipitation with a biocompatible polymer using carbon dioxide as a supercritical fluid antisolvent, J Supercrit Fluids, 88 (2014) 56-65.

[135] J.B. Hall, M.A. Dobrovolskaia, A.K. Patri, S.E. McNeil, Characterization of nanoparticles for therapeutics, Nanomedicine, 2 (2007) 789-803.

[136] R.J. Ahern, J.P. Hanrahan, J.M. Tobin, K.B. Ryan, A.M. Crean, Comparison of fenofibrate-mesoporous silica drug-loading processes for enhanced drug delivery, Eur J Pharm Sci, 50 (2013) 400-9.

[137] R. Campardelli, G.D. Porta, L. Gomez, S. Irusta, E. Reverchon, J. Santamaria, Au-PLA nanocomposites for photothermally controlled drug delivery, J Mater Chem B, 2 (2014) 409-17.

[138] P. M. A. Sherwoord, Auger and X-Ray Photoelectron Spectroscopy, in Handbook of Nanophase Materials, A. Goldstein, Editor. 1997, CRC Press. p. 337-43.

[139] A. Montes, E. Baldauf, M.D. Gordillo, C.M. Pereyra, E.J. Martínez de la Ossa, Polymer encapsulation of amoxicillin microparticles by SAS process, J Microencapsul, 31 (2014) 16-22.

[140] Y. Seo, W. Jhe, Atomic force microscopy and spectroscopy, Reports on Progress in Physics, 71 (2008).

[141] G. Ahuja, K. Pathak, Porous carriers for controlled/modulated drug delivery, Indian J Pharm Sci, 71 (2009) 599-607.

[142] V. Mamaeva, J.M. Rosenholm, L.T. Bate-Eya, L. Bergman, E. Peuhu, A. Duchanoy, L.E. Fortelius, S. Landor, D.M. Toivola, M. Lindén, C. Sahlgren, Mesoporous Silica Nanoparticles as Drug Delivery Systems for Targeted Inhibition of Notch Signaling in Cancer, Mol Ther, 19 (2011) 1538-46.

[143] K. Sing, The use of nitrogen adsorption for the characterization of porous materials, Colloid Surface A, 187 (2001) 3-9.

[144] S. Brunauer, P.H. Emmett, E. Teller, Adsorption of Gases in Multimolecular Layers, J Am Chem Soc, 60 (1938) 309-19.

[145] E. Barrett, L. Joyner, P. Halenda, The determination of pore volume and area distributions in porous substances. 1. Computations from nitrogen isotherms, J Am Chem Soc, 73 (1951) 373-80.

[146] H. Giesche, Mercury porosimetry: A general (practical) overview, Part Part Syst Charact, 23 (2006) 9–19.

[147] B. Kirby, E. Hasselbrink, Zeta potential of microfluidic substrates: 1. Theory, experimental techniques, and effects on separations, Electrophoresis, 25 (2004) 187-202.

[148] L. Rabinovich-Guilatt, P. Couvreur, G. Lambert, D. Goldstein, S. Benita, C. Dubernet, Extensive surface studies help to analyze zeta potential data: the case of cationic emulsions, Chem Phys Lipids, 131 (2004) 1-13.

[149] R. Hidalgoalvarez, On the conversion of experimental electrokinetic data into double-layer characteristics in solid-liquid interfaces. In Advances in Colloid and Interface Science. 1991. p. 217-341.

[150] S. Dalvi, M. Azad, R. Dave, Precipitation and stabilization of ultrafine particles of Fenofibrate in aqueous suspensions by RESOLV, Powder Technol, 236 (2013) 75-84.

[151] R. Muller, C. Jacobs, O. Kayser, Nanosuspensions as particulate drug formulations in therapy Rationale for development and what we can expect for the future, Adv Drug Deliver Rev, 47 (2001) 3-19.

[152] L.N. Hassani, F. Hindré, T. Beuvier, B. Calvignac, N. Lautram, A. Gibaud, F. Boury, Lysozyme encapsulation into nanostructured $CaCO_3$ microparticles using a supercritical CO_2 process and comparison with the normal route, J Mater Chem B, 1 (2013) 4011-19.

[153] I. Sogias, A. Williams, V. Khutoryanskiy, Why is chitosan mucoadhesive?, Biomacromolecules, 9 (2008) 1837-42.

[154] M. Bogatai, T. Vovk, M. Kerec, A. Dimnik, I. Grabnar, A. Mrhar, The correlation between zeta potential and mucoadhesion strength on pig vesical mucosa, Biol Pharm Bull, 26 (2003) 743-746.

[155] S. Patil, A. Sandberg, E. Heckert, W. Self, S. Seal, Protein adsorption and cellular uptake of cerium oxide nanoparticles as a function of zeta potential, Biomaterials, 28 (2007) 4600-07.

[156] S. Salgin, U. Salgin, S. Bahadir, Zeta Potentials and Isoelectric Points of Biomolecules: The Effects of Ion Types and Ionic Strengths, Int J Electrochem Sci, 7 (2012) 12404-14.

[157] E. Frohlich, The role of surface charge in cellular uptake and cytotoxicity of medical nanoparticles, Int J Nanomedicine, 7 (2012) 5577-91.

[158] M. Fraile, R. Buratto, B. Gómez, Á. Martín, M.J. Cocero, Enhanced Delivery of Quercetin by Encapsulation in Poloxamers by Supercritical Antisolvent Process, Ind Eng Chem Res, 53 (2014) 4318-27.

[159] A. Sharma, S. Madhunapantula, G. Robertson, Toxicological considerations when creating nanoparticle-based drugs and drug delivery systems, Expert Opin Drug Metab Toxicol, 8 (2012) 47-69.

[160] N. Lewinski, V. Colvin, R. Drezek, Cytotoxicity of nanoparticles, Small, 4 (2008) 26-49.

[161] B.J. Marquis, S.A. Love, K.L. Braun, C.L. Haynes, Analytical methods to assess nanoparticle toxicity, Analyst, 134 (2009) 425-39.

[162] A.L. Holder, R. Goth-Goldstein, D. Lucas, C.P. Koshland, Particle-Induced Artifacts in the MTT and LDH Viability Assays, Chem Res Toxicol, 25 (2012) 1885-92.

[163] W. Abdelwahed, G. Degobert, S. Stainmesse, H. Fessi, Freeze-drying of nanoparticles: Formulation, process and storage considerations, Adv Drug Deliver Rev, 58 (2006) 1688-713.

[164] A. Bouchard, N. Jovanović, G.W. Hofland, W. Jiskoot, E. Mendes, D.J.A. Crommelin, G.-J. Witkamp, Supercritical fluid drying of carbohydrates: selection

of suitable excipients and process conditions, Eur J Pharm Biopharm, 68 (2008) 781-94.

[165] R. Shaikh, T.R.R. Singh, M.J. Garland, A.D. Woolfson, R.F. Donnelly, Mucoadhesive drug delivery systems, J Pharm Bioallied Sci, 3 (2011) 89-100.

[166] M. Amidi, E. Mastrobattista, W. Jiskoot, W.E. Hennink, Chitosan-based delivery systems for protein therapeutics and antigens, Adv Drug Deliv Rev, 62 (2010) 59-82.

[167] M. Arruebo, R. Fernández-Pacheco, M.R. Ibarra, J. Santamaría , Magnetic nanoparticles for drug delivery, Nano Today, 2 (2007) 22-32.

[168] A. Bootz, V. Vogel, D. Schubert, J. Kreuter, Comparison of scanning electron microscopy, dynamic light scattering and analytical ultracentrifugation for the sizing of poly(butyl cyanoacrylate) nanoparticles, Eur J Pharm Biopharm, 57 (2004) 369-75.

[169] H. Keles, A. Naylor, F. Clegg, C. Sammon, Investigation of factors influencing the hydrolytic degradation of single PLGA microparticles, Polym Degrad Stab, 119 (2015) 228-41.

[170] W. Jiskoot, D. Crommelin, (Eds.), Methods for Structural analysis of Protein Pharmaceuticals, American Association of Pharmaceutical Scientists, USA 2005.

[171] H.-C. Mahler, W. Jiskoot, Analysis of Aggregates and Particles in Protein Pharmaceuticals, John Wiley & Sons, Inc., New Jersey, 2012.

[172] J. das Neves, M. Amiji, M.F. Bahia, B. Sarmento, Assessing the physical-chemical properties and stability of dapivirine-loaded polymeric nanoparticles, Int J Pharm, 456 (2013) 307-14.

[173] K. Moribe, M. Fukino, Y. Tozuka, K. Higashi, K. Yamamoto, Prednisolone multicomponent nanoparticle preparation by aerosol solvent extraction system, Int J Pharm, 380 (2009) 201-5.

[174] A. Argemí, A. Vega, P. Subra-Paternault, J. Saurina, Characterization of azacytidine/poly(L-lactic) acid particles prepared by supercritical antisolvent precipitation, J Pharm Biomed Anal, 50 (2009) 847-52.

[175] M. Kalani, R. Yunus, N. Abdullah, Optimizing supercritical antisolvent process parameters to minimize the particle size of paracetamol nanoencapsulated in L-polylactide, Int J Nanomedicine, 6 (2011) 1101-5.

[176] M. S. Kim, Influence of hydrophilic additives on the supersaturation and bioavailability of dutasteride-loaded hydroxypropyl-β-cyclodextrin nanostructures, Int J Nanomedicine, 8 (2013) 2029-39.

[177] M. Kim, J. Kim, S. Hwang, Enhancement of Wettability and Dissolution Properties of Cilostazol Using the Supercritical Antisolvent Process: Effect of Various Additives, Chem Pharm Bull, 58 (2010) 230-3.

[178] Y. Zu, D. Wang, X. Zhao, R. Jiang, Q. Zhang, D. Zhao, Y. Li, B. Zu, Z. Sun, A novel preparation method for camptothecin (CPT) loaded folic acid conjugated dextran tumor-targeted nanoparticles, Int J Mol Sci, 12 (2011) 4237-49.

[179] E.S. Kolotova, S.G. Egorova, A.A. Ramonova, S.E. Bogorodski, V.K. Popov, I.I. Agapov, M.P. Kirpichnikov, Cytotoxic and Immunochemical Properties of

Viscumin Encapsulated in Polylactide Microparticles, Acta Naturae, 4 (2012) 101-6.

[180] F. Zabihi, N. Xin, J. Jia, T. Chen, Y. Zhao, High Yield and High Loading Preparation of Curcumin-PLGA Nanoparticles Using a Modified Supercritical Antisolvent Technique, Ind Eng Chem Res, 53 (2014) 6569-74.

[181] F. Chen, G. Yin, X. Liao, Y. Yang, Z. Huang, J. Gu, Y. Yao, X. Chen, H. Gao, Preparation, characterization and in vitro release properties of morphine-loaded PLLA-PEG-PLLA microparticles via solution enhanced dispersion by supercritical fluids, J Mater Sci Mater Med, 24 (2013) 1693-705.

[182] M. Araújo, R. Viveiros, T.R. Correia, I.J. Correia, V.D. Bonifácio, T. Casimiro, A. Aguiar-Ricardo, Natural melanin: a potential pH-responsive drug release device, Int J Pharm, 469 (2014) 140-5.

[183] M.S. da Silva, R. Viveiros, P.I. Morgado, A. Aguiar-Ricardo, I.J. Correia, T. Casimiro, Development of 2-(dimethylamino)ethyl methacrylate-based molecular recognition devices for controlled drug delivery using supercritical fluid technology, Int J Pharm, 416 (2011) 61-8.

[184] M. Fraile, ÿ. Martín, D. Deodato, S. Rodriguez-Rojo, I.D. Nogueira, A.L. Simplício, M.J. Cocero, C.M.M. Duarte, Production of new hybrid systems for drug delivery by PGSS (Particles from Gas Saturated Solutions) process, J Supercrit Fluids, 81 (2013) 226-35.

[185] A. Galia, O. Scialdone, G. Filardo, T. Spanò, A one-pot method to enhance dissolution rate of low solubility drug molecules using dispersion polymerization in supercritical carbon dioxide, Int J Pharm, 377 (2009) 60-9.